

Chapter 2

Literature Review

2.1 Introduction

The present work involves the study of layered double hydroxides as CO₂ solid adsorbents with application in sorption-enhanced hydrogen production processes. In this chapter some relevant aspects are addressed including basic background on gas–solid adsorption, CO₂ adsorbents for carbon capture and storage, CO₂ adsorption characteristics of layered double hydroxides and the production of H₂ by sorption-enhancement.

Section 2.2 reviews some basic principles such as the definition of gas–solid adsorption, adsorption isotherms and mass and heat transfer phenomena. Relevant experimental methods to study adsorption (thermogravimetry and breakthrough curve analyses) are briefly explained. In Sect. 2.3 the characteristics of promising types of CO₂ adsorbents are mentioned including their equilibrium capacities and adsorption kinetics, the typical operating window, their performance in the presence of water and their regenerability. Section 2.4 highlights the characteristics and adsorption properties of layered double hydroxides and their derivatives. In addition, different strategies to enhance their performance are presented including the promotion with alkali metals and the use of high surface area materials as supports. In Sect. 2.5 some relevant properties of carbon nanostructures and their potential use as supports are reviewed. Subsequently, Sect. 2.6 describes the industrial production of hydrogen and discusses the relevance of process intensification by sorption-enhancement. Finally, Sect. 2.7 gives some concluding remarks.

2.2 Gas–Solid Adsorption

An increasing interest in gas adsorption processes in chemical and petrochemical industries has been observed since the second half of the last century fostered by numerous scientific and engineering developments such as the discovery of new

porous materials (e.g. carbon molecular sieves and synthetic zeolites) and the invention of clever and novel processes (e.g. more efficient pressure-swing adsorption cycles) [1]. Nowadays, adsorption is of great importance representing not only a key tool for many existing industrial systems but also playing a crucial role in the development of new technologies. A deep understanding of the adsorption phenomena is very important and therefore many books have been written regarding this topic [1–8]. A brief description of some basic adsorption principles will be given in the following subsections.

2.2.1 Basic Adsorption Principles

The term adsorption is used to describe the phenomenon in which molecules of fluid phases, i.e. gases, vapours and liquids (*adsorptive*), enrich the surface of solids (or other liquid phases) forming an interface, that is considered a separate phase from the point of view of thermodynamics [9]. The set of adsorbed molecules (*admmolecules*) on the surface of the solid material is called *adsorbate* whereas the solid phase, usually porous, is named *adsorbent* (Fig. 2.1). The phenomenon of desorption occurs when the adsorbed molecules return to the fluid phase. If the molecular flows to and from the surface are equal then adsorption equilibrium exists, otherwise either adsorption or desorption controls the process [8].

2.2.1.1 Heat of Adsorption

Adsorption phenomena usually exhibit an exothermic behaviour which can be easily explained by simple thermodynamic principles. An adsorbed molecule has less degrees of freedom on the surface of the solid than in the gas phase. As a

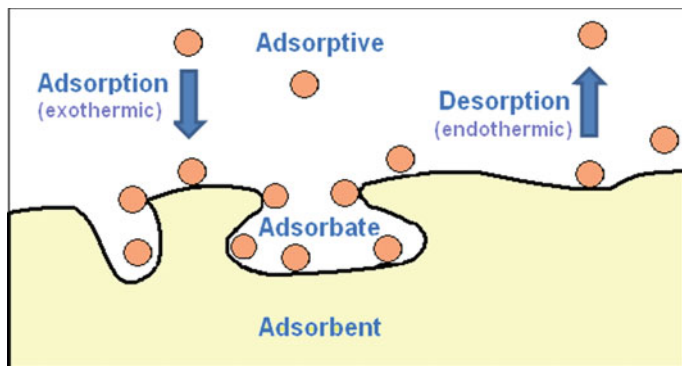


Fig. 2.1 Adsorption system consisting of sorptive gas (adsorptive), a sorbed phase or adsorbate (adsorbate) and a solid sorbent phase (adsorbent) (adapted from Keller [8])

consequence the entropy change caused by adsorption ($\Delta S_{ads} = S_{adsorbate} - S_{gas}$) is necessarily negative. Spontaneous adsorption requires a negative free energy change ($\Delta G_{ads} = \Delta H_{ads} - T\Delta S_{ads}$), hence the enthalpy of adsorption (ΔH_{ads}) must be negative, i.e. the adsorption process is exothermic [3]. This implies that desorption is endothermic.

The heat of adsorption is defined as $Q_{ads} = -\Delta H_{ads}$ and therefore it is a positive quantity. Many definitions of heat of adsorption can be found in the literature [4, 10, 11]. Among them, the isosteric heat of adsorption is very useful for the design of adsorption units. It can be directly measured using calorimetric methods or estimated indirectly from experimental isotherms at different temperatures [10]. From measurements of pressure and temperature at constant coverage θ_i , the isosteric heat of adsorption can be calculated (using van't Hoff equation) as follows:

$$\left[\ln \left(\frac{p_1}{p_2} \right) \right] = \frac{-Q_{ads}}{R} \left(\frac{1}{T_1} - \frac{1}{T_2} \right) \quad (2.1)$$

2.2.1.2 Physical and Chemical Adsorption

A variety of phenomena can be expected to occur during adsorption due to the complex nature of the interactions of the adsorbate with the adsorbent or with co-adsorbed species. Depending on the strength or interaction energy by which admolecules are bound to the surface of the adsorbent, two main types of phenomena can be distinguished: physisorption and chemisorption. In the former, weak intermolecular forces are involved (e.g. van der Waals and/or dispersion forces due

Table 2.1 Basic properties of physisorption and chemisorption phenomena (Ruthven [3], Keller [8])

Property	Physisorption	Chemisorption
Selectivity of adsorptive gases	Non specific	Highly specific
Intensity of adsorption increased for adsorptive gas pressure and temperature	Favoured at high pressure and low temperature	Possible over a wide range of temperatures
Kinetics	Rapid	May be slow
Desorption	Reversible	Irreversible/reversible
Heat of adsorption	Low heat of adsorption (<2 or 3 times the latent heat of evaporation)	High heat of adsorption (>2 or >3 times higher the latent heat of evaporation)
Adsorbate-adsorbent interaction	Monolayer or multilayer, no dissociation of adsorbed species, no electron transfer although polarisation of adsorbate may occur	Monolayer only, may involve dissociation, electron transfer leading to bond formation between adsorbate and surface
Type of phenomenon	Non-activated	Activated/non-activated

to induced dipole-dipole interactions) whereas in the latter, strong bonds are created (e.g. covalent and metallic-type bonding) [11]. Although this distinction is conceptually useful, there are many intermediate cases and it is not always possible to categorise a particular system unequivocally [3]. The general features which differentiate physical and chemical adsorption are summarised in Table 2.1. Most of the industrial separation processes depend on physical adsorption rather than on chemisorption. This is due to the reversible character of physisorption, which allows the adsorbent to be more easily regenerated.

2.2.2 *Regeneration of Spent Adsorbents*

Separation by adsorption is an unsteady process in which regeneration of the adsorbent is needed for cyclic use. The main purpose of regeneration is to restore the adsorption capacity of the spent adsorbent and to recover any valuable component retained. A specific and finite capacity exists for each solid-adsorbate couple at specific temperature, pressure and gas composition. The saturated solids can be regenerated by conveniently changing at least one of these process parameters. Pressure-swing adsorption (PSA) and temperature-swing adsorption (TSA) are among the most used methods to regenerate solid adsorbents [4, 12].

2.2.2.1 Pressure-swing Adsorption

Pressure-swing adsorption processes (PSA) are commonly used for gas-solid systems involving physical adsorption where the regeneration of the adsorbent can be easily done by reducing the total pressure of the bed (i.e. the pressure of the system changes between high pressure during adsorption and low pressure during regeneration). PSA cycles are usually employed when the concentration of the components to be removed is significant (more than a few percent). Under those conditions, the adsorbent is saturated very fast and since the pressure of the system can be changed rapidly, the time between adsorption and regeneration is balanced allowing for a complete cycle in minutes or seconds. PSA technology is widely used in very large scales such as hydrogen recovery, air separation, CO₂ removal, purification of noble gases, CH₄ upgrading and n-iso paraffin separation [1, 5, 12].

2.2.2.2 Temperature-Swing Adsorption

In temperature-swing adsorption (TSA) the solid is primarily regenerated by heating which is usually provided by a purge gas at high temperature. TSA is particularly convenient in the separation of molecules that form strong bonds with the adsorbent. Therefore, this regeneration process has been frequently used to remove components present in relatively low concentrations such as organic solvents from air and moisture from natural gas. In this case, when high product purities are not achievable

with PSA, TSA may be adequate. On the other hand, a challenge of this method is the long duration of the heating-cooling cycles which may adversely affect the cycle productivity. In practice, it is occasionally necessary to combine TSA and PSA cycles to achieve an effective regeneration of the solid [1, 4].

2.2.3 Adsorption Isotherms

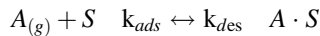
The study of adsorption equilibrium is based on the understanding of adsorption isotherms, which establish the relation between the amount adsorbed and the partial pressure of a species at constant temperature. Isotherms are determined experimentally being usually depicted as a plot of fractional coverage of adsorbate (θ_i) or the amount adsorbed (q_i) versus the relative pressure (p_i/P_o) of the gas. A wide variety of mathematical models have been formulated to interpret different types of isotherms including the equations of Langmuir, Freundlich, Langmuir-Freundlich (Sips), Toth, Temkin, Dubinin and Brunauer-Emmet-Teller (BET). In the following paragraphs the models relevant to the present study are briefly described.

2.2.3.1 Langmuir Isotherm

In 1918, Langmuir proposed the first theoretical model for monolayer adsorption to describe mainly chemisorption phenomena. The basic assumptions of the Langmuir model are: (1) the surface of the adsorbent is homogeneous (i.e. all sites are energetically equivalent), (2) adsorption on the surface is localised (i.e. the molecules are adsorbed on a fixed number of well-defined localised sites), (3) each site can accommodate only one adsorbate molecule and (4) there is no interaction between molecules adsorbed on neighbouring sites [3, 6].

The original model that Langmuir developed was based on the kinetic theory of gases. However, the isotherm can also be derived by other methods including statistical mechanics, thermodynamics and chemical reaction equilibrium [13]. The last approach is relatively simple and useful, and it is developed as follows:

The nondissociative chemisorption of a gas (A) on a site (S) can be represented as:



$$\text{Rate of adsorption} = k_{ads} p_A (1 - \theta_A) \quad (2.2)$$

$$\text{Rate of desorption} = k_{des} \theta_A \quad (2.3)$$

$$\theta_A = \frac{q_A}{m} \quad (2.4)$$

where k_{ads} and k_{des} are the adsorption and desorption rate constants respectively, p_A is the partial pressure of A, q_A is the amount of A adsorbed at a fixed set of temperature and p_A , m is the monolayer capacity (i.e. the amount of A required to completely cover the surface of the adsorbent, which should be independent of temperature) and θ_A is the fractional coverage (dimensionless). At equilibrium the rates of adsorption and desorption are equal:

$$k_{ads}p_A(1 - \theta_A) = k_{des}\theta_A \quad (2.5)$$

Equation (2.5) can be rearranged to obtain the common expression of the Langmuir isotherm:

$$\theta_A = q_A/m = bp_A/(1 + bp_A) \quad (2.6)$$

In Eq. 2.6, $b = k_{ads}/k_{des}$ is the adsorption equilibrium constant. When the partial pressure of A approaches infinity, the fractional coverage tends to 1, while at low adsorbate concentrations ($bp_A \ll 1$), the Langmuir expression reduces to the Henry's law isotherm:

$$\theta_A = q_A/m = bp_A \quad (2.7)$$

The dependence of the adsorption equilibrium constant with temperature follows van't Hoff equation:

$$-RT \ln(b) = \Delta G_{ads} = \Delta H_{ads} - T\Delta S_{ads} \quad (2.8)$$

Therefore b can be expressed as:

$$b = \exp\left(\frac{\Delta S_{ads}}{R}\right) \exp\left(\frac{-\Delta H_{ads}}{RT}\right) = b_o \exp\left(\frac{-\Delta H_{ads}}{RT}\right) = b_o \exp\left(\frac{Q_{ads}}{RT}\right) \quad (2.9)$$

where ΔH_{ads} is the enthalpy of adsorption (negative) and Q_{ads} is the heat of adsorption (positive), which for the Langmuir's model are independent of the coverage. The parameter b , also called affinity constant, is a measure of how strong an adsorbate is attracted onto a surface and decreases with increasing temperature since more energy is provided to desorb the adsorbed molecules.

2.2.3.2 Freundlich Isotherm

In many cases, the assumptions involved in the derivation of the Langmuir model are not adequate to describe real surfaces. Therefore various empirical equations have been proposed to deal with systems that deviate from an ideal behaviour. Among the earliest efforts is the isotherm suggested by Freundlich in 1926, which is expressed as:

$$q_A = k p_A^{1/n} \quad \text{or} \quad \theta_A = k' p_A^{1/n} \quad (2.10)$$

where k and n are generally temperature dependent, decreasing with increasing temperature [14].¹ The parameter n is usually greater than unity and the larger this value is, the more nonlinear the adsorption isotherm becomes [6]. The Freundlich isotherm is expected to be valid only for moderate coverages since the equation does not have a proper Henry's law behaviour at low pressure and it does not have a finite limit when the pressure is very high.

Although this model was proposed originally as an empirical isotherm, it has been justified by thermodynamic and statistical approaches [13, 15]. The theoretical derivation of the Freundlich isotherm considers that the surface of the adsorbent is heterogeneous and can be divided into small domains that contain sites with the same adsorption energy. Each domain is independent from each other (i.e. there is no interaction between domains) and on each domain the adsorbate is adsorbed on one site exclusively. Therefore, the adsorption on a single site within each domain, i , can be described by Langmuir:

$$\theta_i = b_i p_A / (1 + b_i p_A) \quad (2.11)$$

If the b_i values (defined in Eq. 2.9) for each domain are assumed to be distributed continuously, the overall coverage can be written as:

$$\theta = \int \alpha_i \theta_i d_i \quad (2.12)$$

where α_i is the fraction of type i sites and $\alpha_i d_i$ is the frequency of occurrence of θ_i between i and $i + \Delta i$. If it is assumed that the domains i can be represented by the heat of adsorption, Q_{ads} , and that α_i depends exponentially on Q_{ads} then:

$$\alpha_{Q_{ads}} = \alpha_0 \exp(-Q_{ads}/Q_{ads0}) \quad (2.13)$$

where Q_{ads0} and α_0 are constants. Substituting Eqs. (2.13) and (2.11) into Eq. (2.12) and integrating results in the following expression for the coverage:

$$\alpha_{Q_{ads}} = \alpha_0 \exp(-Q_{ads}/Q_{ads0}) \quad (2.14)$$

The fact that $\alpha_{Q_{ads}}$ represents a fractional distribution of adsorption sites requires that $\alpha_0 Q_{ads0} = 1$ [13]. Consequently, Eq. (2.14) can be expressed as $\theta = (b_0 p_A)^{RT/Q_{ads0}}$ which coincides with the empirical Freundlich isotherm (Eq. 2.10). The detailed derivation is given in Appendix A.1.

¹The dependence of k and n on temperature is complex so they should not be extrapolated outside their range of validity. Usually $\ln(k)$ and $1/n$ depend linearly on temperature (Huang and Cho [14]).

2.2.3.3 Toth Isotherm

To broaden the pressure range where the Freundlich model can be applied, other empirical isotherms have been proposed such as the Sips (Langmuir-Freundlich) and Toth equations. The latter isotherm is popular since it is valid at high partial pressures and possesses the correct Henry's law type behaviour at low pressure. The Toth Equation (1971) is a three parameter model and has the following form:

$$q_A = mbp_A / (1 + (bp_A)^t)^{1/t} \quad (2.15)$$

where b and t are specific for each adsorbate-adsorbent pair and depend on temperature [6]. The parameter t is usually less than unity and characterises the heterogeneity of the system. Deviations of t from unity correspond to heterogeneous systems and may stem from the nature of the solid or the adsorbate, or from a combination of both. When $t = 1$, the Toth isotherm reduces to the Langmuir model which represents a homogenous system. Similarly to the Freundlich isotherm, the Toth equation can also be theoretically justified [6]. The Toth model is used to describe experimental adsorption isotherms of hydrotalcite based adsorbents in Chap. 5.

2.2.4 Mass Transfer Phenomena

Before a molecule of gas adsorbs on a solid particle, it must be transported from the well-mixed gas phase to the exterior surface of the adsorbent and, if the material is porous, further into the pore system. External mass transfer resistances exist when a stagnant film of gas is formed around the adsorbent particles creating a concentration gradient between the homogeneous bulk phase and the exterior surface of the solid. On the other hand, if the diffusion inside the adsorbent particles is limited, differences in concentration of the adsorptive gas will develop between the external surface and the interior of the pores.

In the development of mathematical models to describe adsorption in packed columns, it is of great interest to estimate the relative contribution of internal and external phenomena to the overall mass transport. This can be achieved using the *Biot* number, which is a dimensionless quantity that compares the internal and external mass transfer resistances as follows:

$$Bi_m = \frac{\text{internal resistance}}{\text{external resistance}} = \frac{k_m L_C}{D} \quad (2.16)$$

where Bi_m is the mass transfer *Biot* number, k_m is the mass transfer coefficient for the external stagnant film, L_C is a characteristic dimension and D is a term that considers the overall diffusivity of the adsorptive through the pore system [6]. In general, adsorbents operate under conditions where the *Biot* number is large

($Bi_m \gg 1$) and therefore external transfer limitations are usually neglected in the mathematical descriptions [1, 6].

Regarding the resistance to mass transport through the pores, many different diffusion mechanisms may occur simultaneously. Inside very wide pores, the transport is governed by the molecular diffusivity of the adsorptive in the gas mixture. As the pore diameter approaches the mean free path of the gas molecules, interactions with the pore walls become important and the process is controlled by Knudsen diffusion. Additionally, once the molecules are adsorbed, surface diffusion takes place when the adsorbate overcomes the energy barrier to desorb from one adsorption site and hops to an adjacent site. As a consequence, the description of the intraphase transfer requires an expression (D_e , effective diffusivity) that accounts for the different mechanisms that take place during the diffusive transport.

To model adsorption in a packed column, the mass balance within the spherical pellet and for the bulk flow of the bed need to be considered using the following equations [1].

Spherical pellet mass balance:

$$D_e \left(\frac{\partial^2 c_{i_{pore}}}{\partial r^2} + \frac{2}{r} \frac{\partial c_{i_{pore}}}{\partial r} \right) = \frac{\partial q_i}{\partial t} \quad (2.17)$$

Bulk flow mass balance:

$$-D_z \frac{\partial^2 c_{i_{bulk}}}{\partial z^2} + \frac{\partial v c_{i_{bulk}}}{\partial z} + \frac{\partial c_{i_{bulk}}}{\partial t} + \frac{1 - \varepsilon}{\varepsilon} k_m a (c_{i_{bulk}} - c_{i_{surf}}) = 0 \quad (2.18)$$

Continuity at the pellet surface:

$$D_e \left(\frac{\partial c_{i_{pore}}}{\partial r} \right)_{r=R_p} = k_m (c_{i_{bulk}} - c_{i_{surf}}) \quad (2.19)$$

where D_e and D_z are the effective and axial diffusivities respectively ($\text{m}^2 \text{s}^{-1}$); $c_{i_{pore}}$, $c_{i_{bulk}}$ and $c_{i_{surf}}$ are the adsorptive gas concentrations of species i in the pores, the interpellet region and the external surface of the particle respectively ($\text{mol}_{\text{gas}} \text{m}^{-3}$); v is the interstitial velocity (m s^{-1}), ε is the interpellet void fraction; k_m is the average mass transfer film coefficient (m s^{-1}) and a is the exterior surface area of pellets per volume of bed ($\text{m}^2 \text{m}^{-3}$).² However, the solution of these mass balance equations is complicated and demands a tremendous amount of computational time. For this reason, simplifying assumptions are usually made to eliminate the mass balance equation within the adsorbent particles and substitute it by an expression that relates the overall uptake rate to the bulk flow concentrations. Among the most

²In Eq. (2.17) the adsorbate accumulation in the gas phase, $\varepsilon_p \partial c_{i_{pore}} / \partial t$ (where ε_p is the pellet porosity), has been neglected otherwise it appears on the right-hand side.

used approximations for mass transfer rate is the linear driving force model, which is expressed as:

$$\frac{\partial q_i}{\partial t} = k_{LDF}(q_i^* - q_i) \quad (2.20)$$

where q_i is the overall amount of species i adsorbed averaged over the particle volume ($\text{mol}_{\text{gas}} \text{m}_{\text{ads}}^{-3}$), q_i^* is the amount of i adsorbed in equilibrium with the bulk phase concentration, $c_{i,bulk}$, and k_{LDF} (s^{-1}) is a parameter that lumps the different mass transport phenomena that take place within the adsorbent particles. Equation (2.20) replaces Eq. (2.19) and is substituted in the last term on the right-hand side of Eq. (2.18). The pellet mass balance (Eq. 2.17) is thereby eliminated from the model and the resulting material balance Eq. (2.21) can then be solved with the appropriate initial and boundary conditions.

$$-D_z \frac{\partial^2 c_{i,bulk}}{\partial z^2} + \frac{\partial v c_{i,bulk}}{\partial z} + \frac{\partial c_{i,bulk}}{\partial t} + \frac{1-\varepsilon}{\varepsilon} k_{LDF}(q_i^* - q_i) = 0 \quad (2.21)$$

The linear driving force approximation has been widely used to model adsorbers as well as gas separation breakthrough curves, desorption behaviour and cyclic separation processes. In this thesis the LDF model is used to describe the adsorption kinetics of CO_2 -hydrotalcite systems in Chap. 7.

2.2.5 Heat Transfer Phenomena

The effects of heat generation and heat transfer in an adsorptive system need to be taken into account since they affect the adsorption equilibrium and in some cases the adsorption rate. The heat released during transient adsorption gives rise to non-isothermal profiles inside and outside the adsorbent particles. This heat is transferred by conduction between the solid particles and by convection from the adsorbent to the fluid medium; the radiation term is usually neglected. Similar to mass transfer phenomena, there are heat transfer resistances which occur in the external gas film and/or within the particle itself. Depending on which of these limitations are relevant, heat transfer expressions analogous to those written above for mass transfer need to be used [1, 3, 6]. The equations governing heat and mass transport phenomena need to be solved simultaneously to fully describe the adsorption process.

2.2.6 Experimental Methods to Study Adsorption

The continuous progress of adsorption knowledge has led to the development of many experimental methods to study gas–solid adsorption. A consensus to organise

these techniques has not been established yet and therefore many different classifications can be found in the literature [1, 2, 8]. In general they can be grouped either as static or dynamic methods. In the static techniques the gas is brought into contact with the adsorbent in successive doses, either directly or through a capillary. Most of the existing static apparatus (volumetric and gravimetric) are planned to work at low pressure although they can also be designed to work at high pressure [16, 17]. A difficulty associated with these type of methods is that, in order to obtain accurate data, the time required for the equilibration of the system is usually in the order of days. On the other hand, in the dynamic methods the gas flows over the adsorbent for the duration of the experiment. The main advantages of using these transient techniques are that the apparatus are simple and they can be designed to operate over a wide range of pressures and temperatures. In addition, contrary to static methods that usually provide equilibrium data exclusively, information related to the adsorption-desorption kinetics can also be obtained. Among the different dynamic techniques, thermogravimetric analysis (TGA) and adsorption in packed bed columns are relevant for the present research.

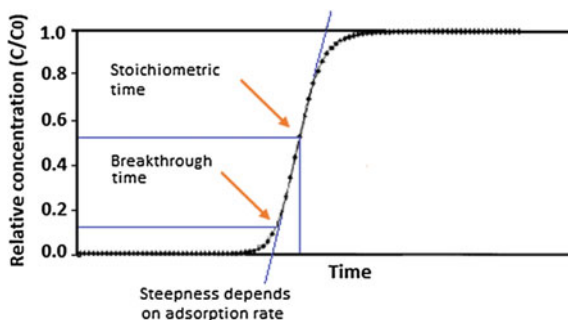
2.2.6.1 Thermogravimetric Analysis

The TGA technique is one of the most practical ways to obtain adsorption data. The amount of gas adsorbed per weight of material (adsorption capacity) is determined by a micro-balance, which measures the weight gain as gas molecules are adsorbed on the solid material (at a particular temperature and partial pressure). Since the changes in weight can be very small, they have to be contrasted always to the sensitivity limits of the instrument so that the reliability of the data can be determined. The method also enables to measure adsorption-desorption kinetics [18, 19], although the parameters obtained are considered to be only estimates of those that correspond to packed bed configurations. This is because usually in the TGA apparatus the gas is flowed past and not through an adsorbent bed, which may slow down the transfer of the adsorptive gas to the active adsorption sites [20].

2.2.6.2 Packed Bed Column

Fixed-bed systems have been widely used to measure gas adsorption on solids due to their relatively easy operation and construction. One of the most common methods to study the dynamics of adsorption columns is to monitor the response of an initially adsorbate free bed to an imposed stimulus in the feed composition of the adsorptive gas. The concentration of the effluent is typically followed by means of a mass spectrometer (MS), infrared spectrometer (IRS), thermal conductivity detector (TCD) or gas chromatograph (GC). The first three detectors allow data to be measured in real time (order of seconds), whereas the frequency of measurements with a GC is usually limited by the time required for the gas sample to pass through the GC column. If the stimulus applied corresponds to a step change, the response is often

Fig. 2.2 Characteristics of a typical adsorption breakthrough curve (adapted from Wood et al. [21])



referred as *breakthrough curve*. This transient profile reflects the progress of the adsorbent saturation and mass transfer zone (MTZ)³ through the column and therefore valuable equilibrium and kinetic information can be extracted from it [3, 4].

A typical breakthrough curve is depicted in Fig. 2.2 and has four distinctive features: (1) the geometric midpoint (stoichiometric time and the corresponding relative concentration), (2) the steepness, (3) the shape and (4) the breakthrough point [21]. The geometric midpoint depends on the superficial velocity of the flowing gas mixture, on the characteristics of the packed bed (size and voidage) and on the adsorption capacity of the material used. The steepness of the elution front is related to the rate at which the adsorptive is removed from the carrier gas. If the overall mass-transfer rate coefficient is large and the approach to equilibrium occurs very rapidly, the breakthrough curve will be very steep while slower uptake rates will give more gradual responses. The shape of the breakthrough curve is determined mainly by the characteristics of the adsorbent. Adsorption on homogeneous surfaces and with constant mass-transfer coefficients along the bed gives symmetrical responses. On the contrary, the asymmetric shape of the breakthrough curves is attributed to the heterogeneity of the adsorbents since the forefront of the adsorption wave will occupy the most active and accessible sites leaving the less active ones for subsequently arriving molecules [21]. The breakthrough point is defined when a fixed concentration of the adsorptive gas emerges in the exit of the column, and the effluent purity no longer meets the specifications of the process.

The geometric midpoint of the breakthrough curve is described by the stoichiometric time. For initially clean adsorbents, the stoichiometric time corresponds to the time at which the bed would be completely saturated if all the adsorptive molecules arrived to all sites simultaneously and the adsorption was instantaneous. It can be calculated by plotting the normalised approach of the effluent to the inlet concentration and integrating over time. That is:

³The term mass transfer zone (MTZ) refers to the section of the column where active adsorption takes place and it is commonly used to classify adsorption systems and to select appropriate models to describe their behaviour [3].

$$t_{st} = \int_{t_0}^{t_{\infty}} (1 - c_i/c_{i_0}) dt \quad (2.22)$$

where t_{st} is the stoichiometric time and c_i and c_{i_0} are the concentrations of adsorptive at the outlet and the inlet of the packed bed respectively. The lower integration limit, t_0 , corresponds to the instant when the step change is done while the upper limit, t_{∞} , is the time necessary so that the feed and the effluent concentrations are equal. The stoichiometric time is often used in expressions to calculate the total adsorption capacity of packed columns [22, 23].

2.2.7 Solid Adsorbent

The selection of a proper porous adsorbent is crucial in all adsorptive processes since good performances in both kinetics and equilibria are required. The kinetic behaviour of the solid is related to the intraparticle diffusion rates of the different adsorbates, whereas the equilibrium is associated with the adsorption capacity of the material and its selectivity towards a particular molecule (depending on the equilibrium affinity). A solid with high capacity but slow kinetics is not suitable since long residence times are needed, i.e. much time is required for the gas to get into the interior of the particle. On the other hand, fast kinetics but small adsorptive capacity is not adequate either as large amounts of material are required for acceptable adsorption yields. Therefore a good adsorbent must have high adsorption capacity and also good kinetics; otherwise low adsorption throughputs are obtained [6].

In order to fulfil the adsorption capacity requirement, the adsorbent must have an adequate micropore volume or specific surface area (generally well in excess of $100 \text{ m}^2 \text{ g}^{-1}$). In addition relatively large pore networks favour kinetics since the diffusing molecules readily reach the micropores in the interior of the particle. This implies that the solid must have a combination of different pore sizes: micropores ($d_{\text{pore}} < 2 \text{ nm}$), mesopores ($2 < d_{\text{pore}} < 50 \text{ nm}$) and macropores ($d_{\text{pore}} > 50 \text{ nm}$) [6, 24].

Besides a suitable porosity, other criteria are essential to select an effective adsorbent. The solid needs to exhibit a reversible adsorption behaviour being stable after repeated adsorption-desorption cycles. Additionally an adsorbent with good mechanical strength is required to work under high pressure. In some systems the hydrophobicity of the materials is very important since the adsorptive gas may contain moisture. Popular commercial solids which usually satisfy these conditions are: alumina, silica gel, activated carbon and zeolites.

2.3 Carbon Dioxide Capture by Solid Adsorbents

As mentioned in Chap. 1, over the past century there has been a dramatic increase in the concentration of CO_2 in the atmosphere, which in turn has made a significant contribution to global warming. The main source of CO_2 associated with human activities is fossil fuel combustion used for power and heat generation and for transportation, which in total accounts for almost 70 % of the global emissions of CO_2 [25]. Unfortunately, an immediate CO_2 -emission halt is not possible since energy demands are expected to increase significantly during the next decades and the so-called green energies are not sufficiently developed to replace fossil fuels on a large scale [26]. As a consequence major technological efforts continue to be devoted to finding suitable processes for carbon dioxide capture and storage (CCS). Gas-solid adsorption is one of the most promising strategies for post-combustion and pre-combustion CO_2 capture applications.⁴ Unlike liquid sorbents, solid adsorbents can be used over a wide temperature range. In addition, CO_2 solid adsorbents that operate at mid- and high- temperatures can be used to enhance the production of H_2 by the so-called sorption-assisted catalytic reactions, which are also regarded as attractive pre-combustion technologies (details are given in Sect. 2.6.1).

An ideal CO_2 adsorbent must fulfil all the conditions mentioned in Sect. 2.2.7. Therefore it must have high selectivity and adsorption capacity for carbon dioxide, fast adsorption-desorption kinetics, adequate multicycle stability and good performance in the presence of water and/or other competing species. In response to these demanding requirements, a range of potential CO_2 adsorbents has been investigated in recent years. Since each has its weaknesses and strengths, the selection of an effective CO_2 adsorbent must be based on giving priority to some criteria so that the constraints of a specific adsorptive process can be met.

All the promising adsorbents that have been identified so far can generally be grouped according to the range of temperature in which they exhibit best performance. Some physisorbents such as zeolites [27–29] and activated carbons [30–32] have been reported to be competitive at temperatures below ~ 393 K. Other materials are also effective at low temperature such as organic-inorganic hybrids (e.g. amines impregnated in silica or covalently bound to silica) [33–35] and an emerging class of adsorbents called metal-organic frameworks [36–38].

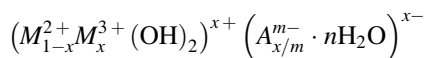
Although some authors have suggested the use of zeolites and activated carbon at temperatures near 523 K [39, 40], some chemisorbents clearly perform better under those conditions. Among these chemisorbents, some undergo surface chemical reactions with CO_2 while others experience bulk chemical reactions. The

⁴In post-combustion CO_2 capture technologies CO_2 is separated from a flue gas after the combustion of a fossil fuel (e.g. the removal of CO_2 from coal-fired power plants). Pre-combustion CO_2 capture refers to processes where CO_2 is removed before the combustion of the fossil fuel (e.g. the fuel is converted to syngas and subsequently to a H_2 -rich stream from which CO_2 is captured).

former group exhibits good adsorption parameters at temperatures between 473 and 773 K (e.g. porous magnesium oxide [41, 42], promoted aluminas [43, 44] and layered double hydroxides [18, 23, 45, 46]), whereas the latter group of adsorbents is suitable in a temperature range from 673 to 973 K (e.g. lithium zirconates [47–49] and calcium oxides [50–52]). Table 2.2 provides a summary of adsorption characteristics of various groups of promising CO₂ adsorbents. In the next section a detailed description of layered double hydroxides (LDHs) is given since these materials are relevant for the present work. LDHs exhibit an adequate multicycle stability and their performance is enhanced in the presence of water. In addition, compared to lithium zirconates and calcium oxides, LDHs show faster adsorption-desorption kinetics and the energy required in their regeneration is significantly lower. Although LDHs show relatively low adsorption capacities, their positive CO₂ adsorption properties and their operating window make them very attractive for some flue gas CO₂ recovery processes and also for sorption-assisted applications such as the sorption-enhanced water gas shift reaction (SE-WGS) and the sorption-enhanced steam methane reforming reaction (SE-SMR) [53–56].

2.4 Layered Double Hydroxides

Layered double hydroxides (LDHs), also known as hydrotalcites (HTs) or mixed-metal layered hydroxides, belong to a large class of anionic clay minerals. Their two-dimensional structure is composed of positively charged brucite-like (Mg(OH)₂) layers in which divalent cations are partially substituted by trivalent cations. These positive ions are located at the centre of octahedral sites of hydroxide sheets, whose vertexes contain –OH anions. Each hydroxyl is shared by three octahedral cations and points towards the interlayer regions. The excess of charge is compensated by negative anions and water molecules located in the interlayer space. This region is highly disordered and its water content depends on the temperature, the water vapour pressure and the nature of the anions present [57]. The neutral structure of the LDH (Fig. 2.3) can be represented by the general formula:



where x is the partial substitution of M^{2+} and M^{3+} and is usually between 0.17 and 0.33 (i.e. M^{2+}/M^{3+} ratios between 2 and 5) [18, 57].

In the natural mineral LDH, the divalent metal is Mg^{2+} , the trivalent cation is Al^{3+} and the compensating anion is CO_3^{2-} with the formula $\text{Mg}_6\text{Al}_2(\text{OH})_{16}\text{CO}_3 \cdot 4\text{H}_2\text{O}$. Although these are the most common ions used in the preparation of synthetic LDHs, a large variety of LDHs have been obtained by using a wide range of metals (e.g. $M^{2+}:\text{Ni}^{2+}, \text{Zn}^{2+}, \text{Cu}^{2+}$ and Mn^{2+} ; $M^{3+}:\text{Fe}^{3+}, \text{Cr}^{3+}, \text{Co}^{3+}$ and Ga^{3+} ; $A^{m-}:\text{SO}_4^{2-}, \text{NO}_3^-, \text{Cl}^-$ and OH^-) [18, 57, 58].

Table 2.2 Summary of the adsorption characteristics of promising CO₂ adsorbents

CO ₂ adsorbent	Type of adsorption	Adsorption temperature (K)	Adsorption capacity (mol kg ⁻¹)	Adsorption-desorption kinetics
(a)				
Zeolites	Mainly physisorption	[298–393]	0.1 < a. c. < 5.5	Fast kinetics described by diffusion models. Equilibrium is achieved in minutes
Activated carbons	Mainly physisorption	[278–348]	0.1 < a. c. < 3.5	Fast kinetics described by diffusion models. Equilibrium is achieved in minutes
Amines impregnated in silica	Mainly chemisorption	[298– 343]	2 < a.c. < 5	Slow kinetics. Equilibrium usually achieved in several hours
Amines covalently bound to silica and organic supports (e.g. carbons, polymers, resins)	Mainly chemisorption	[298–343]	0.1 < a.c < 4 average ~ 1.2	Generally fast initial rate followed by slow rate controlled by diffusion. Equilibrium reached in few hours
Metal-organic frameworks (MOFs)	Physisorption	Room temp. [~298]	max a.c ~3	–
Layered double hydroxides (LDHs)	Physisorption/Chemisorption	[473–773]	0.1 < a.c < 1	Good kinetics described by diffusion models. Equilibrium usually achieved in few minutes/hours
Lithium zirconates	Chemisorption	[673–873]	0.5 < a.c < 6	Slow kinetics. Equilibrium usually achieved in several hours
Calcium oxide	Chemisorption	[723–973]	2 < a. c. < 11.5	Fast initial rate controlled by reaction, followed by slow rate controlled by diffusion. Equilibrium usually achieved in several hours
CO ₂ adsorbent	Regeneration	Effect of steam	Structural modifications/promotion	
(b)				
Zeolites	Easy to regenerate by PSA and TSA [373–573 K]	Usually unfavourable	Alkali and alkaline earth ionic exchange	(continued)

Table 2.2 (continued)

CO ₂ adsorbent	Regeneration	Effect of steam	Structural modifications/promotion
(b)			
Activated carbons	Easy to regenerate by PSA [298 K]	Usually unfavourable	Incorporation of alternative functional groups on the carbon surface (such as amines)
Amines impregnated in silica	Moderate regenerability, usually regenerated by TSA (~343 K) and inert gas purge	Not clear. Generally unfavourable	Different amine loading and method to prepare the support
Amines covalently bound to silica and organic supports (e.g. carbons, polymers, resins)	Good regenerability by TSA (~373 K) and inert gas purge	Favourable	Different amine content and method to prepare the oxide or organic support
Metal-organic frameworks (MOFs)	–	–	Incorporation of amine functionalities giving place to chemisorption sites
Layered double hydroxides (LDHs)	Good regenerability by PSA and TSA [~673 K]	Favourable for adsorption-desorption	Change in framework anions and cations, promotion with alkali metals (e.g. K ₂ CO ₃) and addition of supports
Lithium zirconates	Good regenerability at ~1073 K	Not clear	Morphology and/or crystalline structure modification, addition of alkali components (e.g. Na ₂ ZrO ₃ , K ₂ CO ₃)
Calcium oxide	Rapid degradation during multicycle adsorptive tests. Regeneration by calcination at ~1173 K	Suitable for adsorbent regeneration	Use of rigid supports (e.g. Al ₂ O ₃) and/or additives (e.g. alkali metals), preparation of nanoparticles, use of precursors different from natural CaCO ₃ (e.g. Ca(OH) ₂)

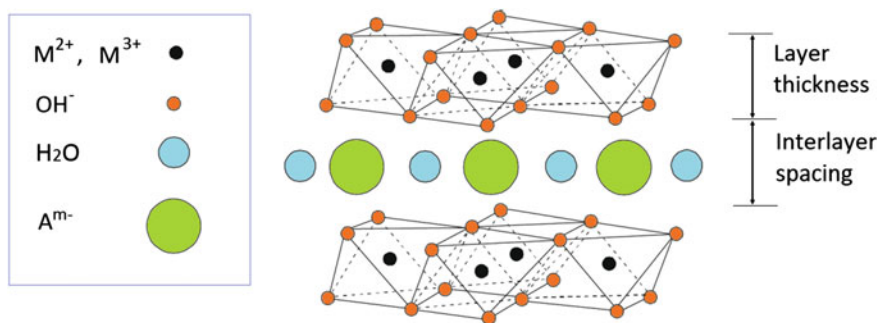


Fig. 2.3 Structure of layered double hydroxides (adapted from Hutson et al. [18])

Layered double hydroxides are typically synthesised by co-precipitation of aqueous solutions of M^{2+} and M^{3+} metal salts⁵ in the presence of the desired interlayer anion. During the preparation of the LDHs, the pH needs to be maintained at higher (or equal) values than that at which the most soluble hydroxide precipitates [59]. Generally a pH range of 8–10 can be used to synthesise most LDHs [60]. The co-precipitation method can be performed under low or high supersaturation conditions. In the former case the two metal salts are added simultaneously to an alkaline solution to maintain the pH constant. On the other hand, in the high supersaturation method the M^{2+}/M^{3+} solution is added to a solution that contains the alkali and the anion precursors. In general, the precipitates obtained by high supersaturation are less crystalline than those produced by low supersaturation since the rate of nucleation tends to be higher than the rate of crystallite growth [59]. For both methods, co-precipitation is followed by a thermal treatment to enhance the yield and the crystallinity of the LDH. Besides co-precipitation, other methods have been used to synthesise LDHs such as the urea and sol-gel techniques [59–62].

Besides the potential application of LDHs as CO_2 adsorbents, their basic properties make them attractive for many catalytic reactions such as self-condensation, cross-aldol condensation of aldehydes and ketones, Michael addition, transesterification and alkylation. Additionally, they have a good anion-exchange capacity and therefore they are used as ion-exchangers and sensors. As mentioned above, LDHs can be prepared with many reducible divalent (e.g. Ni, Cu, Co) and trivalent cations (e.g. Fe, Cr) in the structure which give them suitable redox properties. The intimate contact between the metallic components of the LDHs that is achieved after calcination allows these structures to be used as precursors for the preparation of mixed oxides active for oxidation, hydrogenation and dehydrogenation reactions [63].

⁵Metal nitrate and chloride salts are commonly used due to the low selectivity of LDHs towards these anions [59].

2.4.1 Effect of Thermal Treatment on the Structure of Layered Double Hydroxides

Due to their relatively low basicity, as-synthesised LDHs are often inactive for CO_2 adsorption at high temperature and in many catalytic reactions. The poor basic character of fresh LDHs is mainly caused by the presence of adsorbed water which hinders the access of the adsorptive/reactive gas to the basic sites located on the surface and on the interlayer region [63]. Therefore hydrotalcites often need to be activated by a thermal treatment before being used. Typically LDHs are calcined in nitrogen or air between 673 and 823 K for at least 4 h [61, 64–66]. During this treatment, Mg–Al LDHs are transformed into layered double oxides (LDOs), which are well-dispersed $\text{Mg}(\text{Al})\text{O}$ mixed oxides with a high surface area that stems from the formation of significant porosity [67]. Although XRD measurements have shown that these derivatives are amorphous [61], SEM and TEM images have revealed that they usually maintain the morphology of the original precursor [68]. The use of excessive calcination temperatures leads to the appearance of spinel phases (MgAl_2O_4), which commonly should be avoided in order to preserve the platelet morphology of LDHs and an adequate basicity [63]. Costa et al. [65] found that a calcination temperature of 673 K produces LDOs with an optimum balance between basic sites and surface area which maximises their CO_2 adsorption capacity at temperatures above 473 K. It is worth mentioning that when LDOs are rehydrated, the double layers are partially reconstructed to produce meixnerite ($\text{Mg}_6\text{Al}_2(\text{OH})_{18} \cdot 4\text{H}_2\text{O}$), Fig. 2.4 [69]. This structure exhibits mild Brønsted basicity and is an efficient catalyst in many organic reactions such as self- and cross-aldol condensation of aldehydes and ketones [70–73].

Numerous studies have investigated the structural changes that LDHs experience with temperature [65, 67, 74–76]. Hibino et al. [74] published a detailed study investigating the decarbonation behaviour during heat treatment of a LDH sample with a $\text{Al}/(\text{Mg} + \text{Al})$ ratio equal to 0.33. Five main peaks, corresponding to the release of adsorbed molecules, were observed in the range of 298–1273 K. The first peak appeared below 473 K, and did not affect the integrity of the double layered structure. However the material was partially dehydrated and a significant rearrangement of the octahedral brucite-type layer occurred. The Al^{3+} cations migrated out of the layer to tetrahedral sites in the interlayer producing a decrease in the

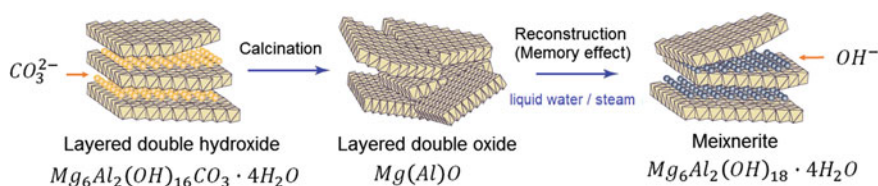


Fig. 2.4 Activation of LDH by thermal treatment followed by reconstruction (adapted from Tichit and Coq [71])

d spacings which progressed with temperature. The second peak was identified between 473 and 623 K. In this range of temperature the dehydroxylation of OH bonds with Al^{3+} occurred and the layered structures collapsed. The third peak became visible at ~ 623 K and corresponded to the maximum CO_2 evolution from the solid. At this temperature the material was completely dehydrated and partially dehydroxylated giving place to a high surface material ($\sim 200 \text{ m}^2 \text{ g}^{-1}$). The authors confirmed by IR analysis that at 773 K, the carbonates that were still present on the solid represented 20 % of the total original value. The remaining carbonates evolve in two overlapping peaks centred at 873 and 1173 K. The release of these carbonates coincides with the migration of Al^{3+} to MgO , which leads to the formation of spinel structures (MgAl_2O_4). This fact suggests that the carbonates are coordinated with Mg^{2+} cations and this coordination is affected by the Al^{3+} ions migration.

2.4.2 *Factors Impacting on the Basicity of Layered Double Hydroxides*

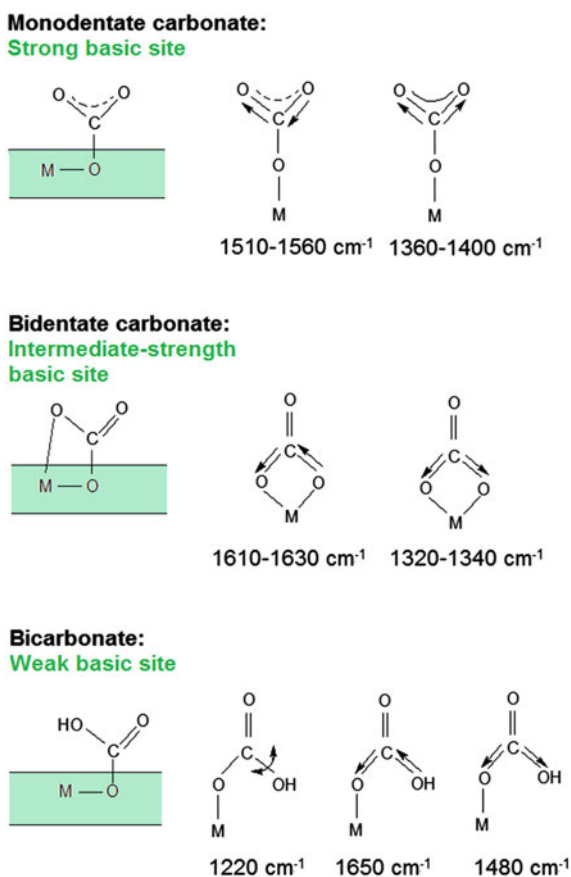
As mentioned before, layered double hydroxides have an ordered structure in which layers formed by divalent and trivalent cations are separated by anions and water molecules. These materials behave as solid bases and, depending on their composition and on the pretreatments that they are subjected to, a wide range of basic densities and strengths can be obtained. As-synthesised and reconstructed LDHs usually present very weak Brønsted basicity which is mainly dictated by the nature of the intercalated anion (CO_3^{2-} , NO_3^- , Cl^- , SO_4^{2-}) and by the amount of remaining water. After calcination, the compensating ions and water are released and the resulting highly defective layered double oxides (LDOs) exhibit much higher (Lewis type) basicity than the fresh LDHs. In consequence, the basicity of the LDHs increases with the calcination temperature up to 923 K, when phase segregation and spinel (MgAl_2O_4) formation occur [63].

There are many factors that influence the basicity of layered double oxides. Although some weak basicity from remaining hydroxyls may exist in the calcined materials, the nature and the relative amount of the divalent and trivalent cations are the main factors that govern the basicity of the mixed oxides. In general, both metal ions must have radii close to 0.65 \AA to form stable structures but small variations in the size produce significant differences in the strength of the basic sites [63]. Low charge-to-radius ratios of the cations result in higher negative charge densities located on the linking oxygen atoms rendering stronger bases. In the particular case of Al^{3+} and Mg^{2+} , aluminium oxide is an amphoteric material with higher heats of adsorption for NH_3 ($\sim 130 \text{ kJ mol}^{-1}$) than for CO_2 ($\sim 70 \text{ kJ mol}^{-1}$) while magnesium oxide chemisorbs CO_2 exclusively with an initial heat of adsorption of 120 kJ mol^{-1} [77]. Compared to the basicity of MgO , LDOs exhibit lower basic density but stronger sites which are attributed to the introduction of aluminium in

the structure. Although the nature of this synergy is still a matter of discussion, it seems that the addition of aluminium increases the number of surface defects and tends to decrease the size of the LDO crystallites [71].

Carbon dioxide has enough acidity to chemisorb even on the weakest basic sites of the layered double oxides. Temperature-programmed desorption monitored by IR spectroscopy [78, 79] conducted over LDOs calcined at 773 K shows that CO_2 coordinates weakly with surface hydroxyl groups to form surface bicarbonate anions. Adsorption sites of intermediate strength correspond to bidentate carbonates coordinated to acid-base pairs such as $\text{Mg}^{2+}\text{--O}^{2-}$ or $\text{Al}^{3+}\text{--O}^{2-}$. The strongest basic sites are monodentate carbonates that appear over low coordination (isolated) oxygen anions associated with defective surfaces [63, 80]. The adsorbed CO_2 species on LDOs are depicted in Fig. 2.5. The promotion of layered double oxides with alkali metals is a common strategy to tune their basicity for gas-phase adsorption applications. The presence of monovalent alkali ions such as sodium and potassium increases considerably the number of basic sites in the resulting LDO as well as the relative proportion of monodentate to bidentate carbonates [63].

Fig. 2.5 Adsorbed CO_2 species on LDH and their corresponding IR signals (adapted from Di Cosimo et al. [79])



2.4.3 *Strategies to Improve the Adsorption Performance of Layered Double Hydroxides*

An adequate CO₂ adsorption performance requires high equilibrium capacities, fast kinetics and good regenerability. While layered double hydroxide derivatives (i.e. layered double oxides) exhibit outstanding kinetics compared to other materials that adsorb CO₂ in the same temperature range, their capacity and multicycle stability need to be further improved before technologies based on LDOs are industrially implemented. Different strategies have been explored to overcome these limitations including the substitution of framework metals or the promotion with alkali metals to increase their capacity, and the addition of water in the feed to enhance their capacity and regenerability. Additionally, it has been reported that dispersion on different supports increases the amount of CO₂ that can be adsorbed per mass of LDO. In the present section, the most common methods to enhance the adsorption performance of hydrotalcite derivatives are reviewed.

2.4.3.1 Substitution of Framework Metals

Numerous studies have attempted to increase the adsorption capacity of Mg–Al–CO₃ LDOs by substituting the structural ions. Tsuji et al. [81] synthesised a range of LDOs with different divalent cations (e.g. Mg, Cu, Zn, Ni and Co) and found that the Mg–Al–CO₃ and Co–Al–CO₃ LDOs showed the highest CO₂ uptake (~ 0.4 mol CO₂ kg⁻¹ at 298 K and $p_{\text{CO}_2} = 66$ mbar). Rodrigues et al. [75] investigated the effect of the type of compensating anion and concluded that lower adsorption capacities were obtained with OH⁻ compared to CO₃²⁻ (0.1 and 0.2 mol CO₂ kg⁻¹ respectively at 573 K and $p_{\text{CO}_2} = 50$ mbar). Hutson et al. [18] assessed the CO₂ adsorption properties of Mg/Al and Ca/Al LDOs with different anions including CO₃²⁻, Fe(CN₆)⁴⁻, Cl⁻ and ClO₄⁻. Among all the samples studied, a synthetic LDO with the formula of the natural mineral hydrotalcite exhibited the fastest kinetics and the highest adsorption capacity (0.6 mol CO₂ kg⁻¹ at 573 K and $p_{\text{CO}_2} = 1000$ mbar). White et al. [82] and Yavuz et al. [83] improved the adsorption capacity of LDOs by partially or totally replacing Al with Ga, La or Ce. More recently, Wang et al. [84] investigated the effect of different trivalent cations (Al, Fe, Ga and Mn) on the CO₂ adsorption performance of LDOs containing Mg²⁺ and CO₃²⁻. The authors demonstrated that the type of trivalent cation used determines the structure evolution of LDH derivatives during thermal treatment and consequently influences their CO₂ capacity.

In addition to framework metal substitution, extensive research has been focused on increasing the CO₂ capacity of Mg–Al LDOs by varying the Mg²⁺ to Al³⁺ ratio [62, 75, 85, 86]. However, there has been little agreement regarding the optimum ratio which seems to be highly dependent on the specific conditions used during the thermal treatment and the CO₂ adsorption. In general, Mg/Al ratios in the range of 1 to 3 have been shown to be suitable for CO₂ adsorption at high temperature.

2.4.3.2 Alkali Promotion of Layered Double Hydroxides

The promotion of layered double hydroxides by alkaline dopants is one of the most practical ways to enhance their CO₂ adsorption capacity. As mentioned earlier, the presence of alkali ions (e.g. sodium, potassium and caesium) increases significantly the number and strength of basic sites in the LDHs. Alkali metals are often added to the LDHs by conventional impregnation methods but can also be incorporated by leaving residues from the coprecipitation agents (e.g. NaOH, KOH, Na₂CO₃ and K₂CO₃) [61, 87, 88].

Most of the research concerning alkali based LDHs has focused on investigating the adsorption properties of potassium promoted hydrotalcites and their application to sorption- assisted reactions such as the SEWGS and the SESMR [23, 54, 55, 85, 89–92]. Reijers et al. [85] assessed the CO₂ adsorption performance of a series of unpromoted and potassium promoted Mg–Al LDHs to be used in SESMR. The authors found that the CO₂ uptake at 673 and 773 K was significantly higher for the K-LDH samples but was practically insensitive to the potassium carbonate loading in the adsorbent, which was varied between 11 and 44 wt%. Rodrigues et al. [90] reported that the adsorption capacity of LDHs was considerably enhanced by promoting them with potassium and caesium. Since the surface area of the alkali loaded adsorbents was found to be much lower than that of the alkali free LDHs, they concluded that the increase in the CO₂ uptake was not directly related to the porosity of the sample but to the presence of additional interactions with or aided by the alkali cations. Walspurger et al. [91] investigated the type of active species responsible for the CO₂ adsorption on potassium promoted LDHs under conditions relevant to the SEWGS. They demonstrated that potassium ions strongly interact with the aluminium oxide centres in the LDH and this generates basic sites which reversibly adsorb CO₂ at 673 K.

2.4.3.3 CO₂ Adsorption in the Presence of Water

It has been widely reported that the presence of water has a positive influence on the CO₂ adsorption performance of activated layered double hydroxides. Ding et al. [45] studied the effect of steam on the adsorption and desorption steps of a pressure swing process using a potassium promoted LDO. They found that the adsorption capacities of the K-LDO at 673 and 753 K were ~10 % higher under wet conditions compared to those obtained under dry conditions. Additionally, the multi-cycle stability of the adsorbent was significantly better in the presence of water. Remarkably, the partial pressure of water was found to have little effect on the adsorption capacity, which suggested that even low concentrations of steam are able to further activate the adsorption sites possibly by maintaining the hydroxyl concentration of the surface and/or preventing site poisoning through carbonate or coke deposition. In a subsequent work, Ding et al. [93] demonstrated that K-LDOs exhibit good adsorption performance even in the presence of considerably high concentrations of water (30 % v/v of water).

In a more recent study, Costa et al. [94] corroborated the findings published by Ding et al. showing that the CO₂ capacity at 473 K and the stability after TSA cycling of unpromoted LDOs were considerably enhanced by adding steam to the gas feed. The authors suggested that in the presence of carbon dioxide and water MgO and Al₂O₃ form bicarbonate species, Mg(HCO₃)₂ and Al(HCO₃)₃ which are responsible for the increased CO₂ uptake observed. Rodrigues et al. [75] reported that the presence of molecular water in the structure of the LDOs also favours their adsorption capacity. Similarly to Costa et al., they attributed the observed enhancement to the formation of bicarbonate species.

Regarding other competing species, it has been observed that K-promoted LDOs are able to coadsorb H₂S without affecting their CO₂ capacity significantly. It was proposed that the adsorption of sulphur occurs on two different types of sites: in some of them H₂S and CO₂ compete for adsorption although the affinity is higher for CO₂, while others adsorb H₂S exclusively, possibly as metal sulphides. Therefore, LDOs can be used in processes that involve the treatment of sour streams [95].

2.4.3.4 Supported Layered Double Hydroxides

Recently, it has been reported that the intrinsic capacity of activated LDHs (i.e. the amount of CO₂ adsorbed per mass of LDO) increases when they are dispersed over materials with high surface area. Although to date there are few works addressing this effect, it is expected that more active LDH derivatives will be obtained following this novel approach. The beneficial role of the support on the capacity of LDOs may stem from the stabilisation of smaller and more defective crystals, and from an increased accessibility of CO₂ to the adsorption sites. As mentioned above, the basicity of LDOs is a size-dependent characteristic since strong sites are associated with low coordinated O²⁻ anions which are present at the corners and the edges of the crystallites. Consequently, it is important to identify supports that are able to stabilise LDHs and that prevent sintering during multicycle operation.

Othman et al. [96] reported that zeolites coated with LDHs (Mg:Al ratio of 3) exhibit almost double the CO₂ adsorption capacity of uncoated LDOs in a temperature range from 303 to 573 K [62]. However, since the zeolites used are CO₂ adsorbents themselves, especially at low temperature, it is difficult to assess the influence of the support on the intrinsic capacity of the LDH derivatives. Aschenbrenner et al. [97] combined LDHs with bohemite alumina consisting of 50:50 LDH:alumina by weight and observed an enhancement of the thermal stability and adequate capacities (between 2 and 2.5 mol CO₂ kg⁻¹ at 293 K), which were found to be independent of the divalent to trivalent cation ratio. The most notable improvement in the intrinsic capacity of LDOs (per mass of LDO) was reported by Meis and co-workers [80]. These authors found that the intrinsic capacity of unsupported LDOs was increased by an order of magnitude (1.3–2.5 mol CO₂ kg⁻¹ at 523 K) when supported on a large fraction of carbon nanofibers (CNF) matrix (82–97 wt% CNF) and in the presence of water. They also showed

that the addition of potassium to the CNF-supported materials results in even higher CO₂ capacities [88].

Although the use of supports appears to be effective for the improvement of the intrinsic sorption performance of LDOs, there are some drawbacks associated with this strategy. The main disadvantage is that so far, the increase in the intrinsic capacity of the layered oxides has been observed only when the crystallites are very well dispersed. This requires very high loadings of support which decreases the CO₂ capacity per total volume of adsorbent (LDO + support) and results in larger sorption units with higher overall costs. Consequently, the identification of supports that maximise the stability and the adsorption capacity of LDOs at relatively low loadings is crucial for industrial applications.

2.5 Carbon Nanostructures as Supports

The high surface area and porosity of some forms of carbon have awakened interest on their use as solid adsorbents or as supports in heterogeneous catalysis. Graphitic carbon exhibits a remarkable mechanical resistance and high stability in acidic and basic media. Additionally, the dispersion of the active phase is relatively easy compared to other supports. Until now there are few industrial processes that employ carbon as a support and only activated carbon or carbon blacks have been used so far [98]. However, nanostructured forms of carbon offer the possibility to improve diffusion due to larger intraparticle voids and therefore to fully exploit the high surface area of these materials [99].

Graphitic crystalline structures are obtained by combining carbon atoms having sp² hybrid orbitals. This configuration results in three σ -bonds localized along the plane connecting the carbon atoms which are arranged in a honeycomb 2D lattice known as *graphene*. The remaining 2p_z free electrons are weakly held to the nuclei and are distributed normal to the plane connecting the carbon atoms. The σ -covalent bonds are responsible for the great strength and mechanical properties of graphene while the delocalized 2p_z electrons are responsible for its electronic properties [100]. Two-dimensional graphene is considered to be the building block of several carbon allotropes. For instance, when many layers of graphene (typically more than three) are stacked one on top of the other, the three dimensional structure of *graphite* is obtained. Alternatively, graphene sheets can wrap forming hollow cylindrical structures known as *single-walled carbon nanotubes (SWCNTs)* with a diameter that ranges from about 0.5–5 nm and a specific surface area of 1315 m² g⁻¹, Fig. 2.6. When many graphene layers (from two to tens) arrange in concentric cylinders, *multi-walled carbon nanotubes (MWCNTs)* are obtained. MWCNTs have outer diameters in the range of 1.4–100 nm and surface areas between 700 and 800 m² g⁻¹ [101].

Graphene and carbon nanotubes are usually synthesised by chemical vapour deposition using Ni, Fe or Cu as catalysts. The nucleation and growth usually occurs by exposure of the transition metals to CO or to a hydrocarbon gas at

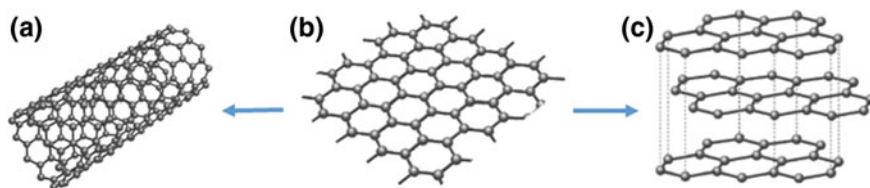


Fig. 2.6 Illustration of single-walled nanotube (a), graphene (b) and graphite (c)

temperatures around 1000 K and low pressures. Alternatively, graphene layers can be produced by oxidation of graphite followed by chemical and thermal exfoliation to produce *graphene oxide* sheets [102]. In graphene oxide, part of the carbon atoms change hybridization to sp^3 to combine with hydroxyls and peroxides in the basal planes, and with carbonyl and carboxylic groups that are located at the edges [103]. An important property of graphene oxide is that it can be easily dispersed in water and other organic solvents, which makes it an attractive support for various materials such as polymers and ceramics. The as-synthesised graphene, graphene oxide and CNTs are often contaminated with residues of the metal precursors and with undesirable by-products such as amorphous carbon. To remove these impurities, the materials are often treated with oxidants such as HNO_3 , H_2SO_4 and $KMnO_4$. This purification treatment introduces acidic functionalities (i.e. $-COOH$, $-C=O$, and $-OH$) which help to solubilise the carbon structures in aqueous media. Additionally, these attached oxidic groups play an important role in the synthesis of composite supported materials (adsorbents and catalysts), providing strong fiber-matrix bonding and thus improving their mechanical properties [101].

2.6 Perspectives on Hydrogen Production

Hydrogen has a wide range of applications in the chemical and petrochemical industries, being used to produce principally ammonia, refined petroleum products and a large variety of chemicals. In addition, it is used in the metallurgic, electronic, and pharmaceutical sectors. Excluding the aeronautic industry, hydrogen has rarely been used as a fuel [104]. However, recently it has been considered as a promising source of clean energy and therefore much research is focused on developing a hydrogen sustainable economy. Unlike fossil fuels, hydrogen burns cleanly, without emitting any environmental pollutants such as carbon dioxide.

Hydrogen is not a primary energy source, but rather an energy carrier. It must be first manufactured before it can be used as a fuel. Industrially, hydrogen is mainly produced from fossil fuels natural gas being the major contributor. Methane is converted to hydrogen by steam reforming (SR) or by partial oxidation with oxygen (PO), or by both in sequence, i.e. autothermal reforming (AR). Although partial oxidation and autothermal reforming are more efficient than simple steam

reforming, the latter is preferred since it does not involve the presence of oxygen which gives rise to additional production costs [105].

The steam reforming process consists in the reaction of sulphur-free natural gas with steam over a nickel-based catalyst at high temperatures and pressures (1073–1173 K and 5–35 bar, respectively) [106]. The water gas shift reaction (WGS) also takes place to some extent and therefore the product stream contains important amounts of water gas (H_2 , CO, CO_2 , H_2O) and unreacted CH_4 . Since these reactions are equilibrium limited, additional water gas shift reactors are placed after the reformer to increase the overall hydrogen yield. The first WGS reactor operates at 573–773 K whereas the second operates near 473 K. Typically, a chromium-iron oxide catalyst is used in the high temperature reactor and a copper-zinc catalyst in the low temperature reactor. Finally, different purification processes (e.g. pressure swing adsorption, amine scrubbing, methanation and preferential oxidation) are used to eliminate carbon dioxide, unreacted carbon monoxide and other impurities, Fig. 2.7. The selection of these purification processes depends on the final purity required [107].

Besides natural gas, hydrogen can be produced from coal by the so-called integrated gasification combined cycle (IGCC). This technology is very energy efficient allowing the co-generation of hydrogen and electricity. In this process, coal is gasified by partial oxidation with oxygen and steam at high temperature and pressure. The resulting synthesis gas (mainly CO and H_2 , but also CO_2) is further reacted with steam to enhance the hydrogen yield by the WGS. Next, the gas is cleaned to recover hydrogen, Fig. 2.7. Regrettably, due to the low hydrogen to carbon ratio of coal, the amount of CO_2 emitted per unit of H_2 (or energy) is large compared to combined cycles based on methane or oil, and this has limited the implementation of coal processes. A current challenge is then to couple IGCC with systematic carbon dioxide capture and sequestration processes [104].

An innovative energy efficient technology to increase the hydrogen production in chemical industry has been recently patented by Haldor Topsøe [108]. This process, called methanol-to-shift, is carried out in a water gas shift reactor feeding

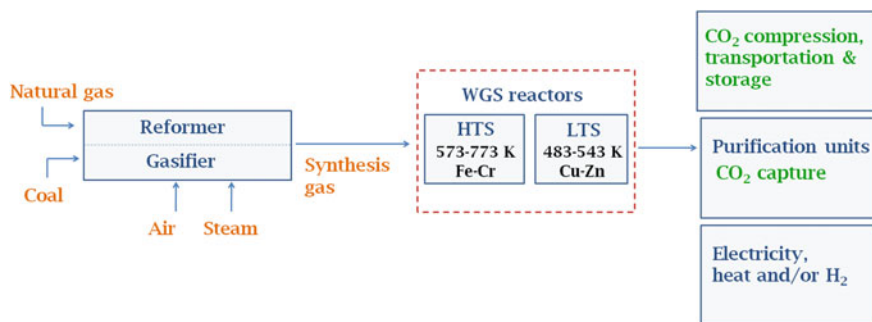


Fig. 2.7 Typical stages of the process of hydrogen production from natural gas (reforming) or coal (gasification)

simultaneously synthesis gas (mainly CO and H₂), water and methanol. A catalyst containing copper, zinc and aluminium enables hydrogen production from both CO shift conversion and methanol decomposition at operating conditions near 553 K and 20 bar. Further understanding of methanol-to-shift is needed since until now few studies have been published in the open literature [108, 109].

Small-scale hydrogen production can be performed via steam reforming, partial oxidation and autothermal reforming of hydrocarbons such as methane, methanol and ethanol. Although these technologies are more expensive and less efficient compared to large industrial processes, they avoid the cumbersome and dangerous transportation of hydrogen from distant centralized production centres. In addition, these processes can be coupled with small purification units to provide a hydrogen rich feed gas for fuel cells applications.

In recent decades new environmentally friendly processes, based on renewable sources rather than on fossil fuels, have been in continuous development to cover the increasing global demand of hydrogen. Important examples of these future technologies are the water electrolysis by alternative energies, photolysis (photo-electrochemical and photobiological) and biomass conversion. Regarding this last technology, biomass can be transformed into hydrogen by gasification or pyrolysis. In addition it can be used for the production of liquid fuels such as ethanol, methanol and glycerol (a major product of biodiesel), which subsequently can be transformed to hydrogen by steam reforming reactions [104, 105].

2.6.1 Sorption-Enhanced Hydrogen Production

Sorption-enhancement refers to intensified processes in which catalytic reactions are coupled with in situ separation by adsorption. These configurations may significantly improve the reactant conversion or/and the product selectivity. According to the Le Chatelier's principle, the removal of one of the products can shift the reaction equilibrium towards more favourable conditions than those achieved under conventional reaction operation. Adsorption-reaction systems enable lower operating temperatures reducing the energy demand of the process and preventing catalyst fouling (e.g. by carbon deposition). In addition, capital cost can be reduced due to process simplifications such as the use of less complicated purification units and the elimination of additional reactors used to enhance the conversion of an equilibrium limited reactor [107, 110].

In sorption-enhanced processes, the catalyst is usually physically admixed with the adsorbent and placed into the adsorptive reactor. Hence both solids and their relative quantities need to be carefully selected since adsorption and reaction kinetics must match under the same operating conditions. After the adsorbent is saturated it needs to be regenerated. If the regeneration conditions do not deactivate the catalyst, the adsorbent recovery can be carried out in two fixed-bed reactors, one operating in the adsorption-reaction mode and the other in the regeneration mode.

Otherwise, more complex engineering is required involving transported or fluidised systems [107].

Sorption-enhanced hydrogen production has been suggested to be feasible for methane steam reforming [53, 54, 107, 111–113], water gas shift reaction [55, 56, 95, 114–116], steam gasification of biomass [117, 118], and more recently for glycerol steam reforming [119, 120] and ethanol steam reforming [121–123]. In general the production of H_2 involves two primary reactions: the endothermic steam reforming and the moderately exothermic water gas shift (see Fig. 2.7). Since both reactions are thermodynamically limited, the in situ removal of carbon dioxide by a selective solid adsorbent displaces the reaction equilibrium and therefore almost complete conversion can be achieved. Although the main target of sorption-enhancement in the production of H_2 is to increase the amount of H_2 produced, the fact that CO_2 is removed simultaneously make the assisted process attractive as a pre-combustion CO_2 capture technology.

In the case of the sorption-assisted steam reforming process, more favourable thermodynamics allows for lower operating temperatures, which decrease the energy consumption and mediate the catalyst deactivation by coke formation. In addition, the water gas shift stage that usually follows the reformer may not be required, making the final purification of hydrogen simpler. Regrettably, a closer

Table 2.3 Sorption-enhanced processes for H_2 production

SE- H_2 process	Main reaction	Operating conditions (K) ^a	CO_2 adsorbents	Catalysts
Methane steam reforming	$CH_{4(g)} + H_2O_{(g)} \leftrightarrow 3H_{2(g)} + CO_{(g)}$	673–873	CaO [50, 107, 112] LDHs [53, 54, 85, 107, 111] Li_2ZrO_3 [107, 113] Na_2ZrO_3 [107, 113]	Ni based
Water gas shift reaction	$CO_{(g)} + H_2O_{(g)} \leftrightarrow H_{2(g)} + CO_{2(g)}$	573–873	CaO [115, 116] LDHs [55, 56, 95, 114]	Fe–Cr Pt-ZDC ^b
Steam gasification of biomass	$C_nH_mO_p(g) + (2n-p)H_2O_{(g)} \leftrightarrow (m/2 + 2n-p)H_{2(g)} + nCO_{2(g)}$	673–973	CaO [117, 118]	Ni based
Glycerol steam reforming	$C_3H_8O_{3(g)} + 3H_2O_{(g)} \leftrightarrow 7H_{2(g)} + 3CO_{2(g)}$	673–973	CaO [119, 120]	Ni based
Ethanol steam reforming	$C_2H_6O_{(g)} + 3H_2O_{(g)} \leftrightarrow 6H_{2(g)} + 2CO_{2(g)}$	773–973	CaO [121–123]	Ni based

^aA wide range of pressures has been recommended, in general: 1–50 bar

^bZDC zirconia-doped ceria

analysis of the sorption-enhanced steam methane reforming (SESMR) reveals that in order to obtain adequate CH_4 conversions, extremely low CO_2 concentrations in the gas phase are required which are difficult to achieve in practice [124]. For instance, at 673 K and 1 bar, only 270 ppm of CO_2 are tolerated if conversions above 90 % are targeted, but the restrictions are even more severe if the process operates at higher pressures (10 ppb at 17 bar). On the other hand, the CO_2 adsorption requirements for the water gas shift are not so demanding and therefore the enhanced process is more feasible. Instead of having two shift reactors in series operating at high and low temperatures, sorption-enhanced water gas shift (SEWGS) requires only one reactor at intermediate temperature, where fast kinetics assisted by adsorption potentially results in smaller units.

Different chemisorbents such as calcium oxide, hydrotalcites and to a lesser extent lithium zirconates have been suggested as promising candidates for sorption-enhanced hydrogen production. Table 2.3 shows a summary of the mentioned hydrogen sorption-enhanced processes and the corresponding recommended adsorbents.

2.7 Concluding Remarks

The growing demand for ammonia derivatives and the need to process heavier petroleum feedstocks have generated great interest in the development of new processes for hydrogen production aiming to be more economic and environmentally friendly. In this regard, sorption-enhancement is a promising technology to improve the efficiency of processes in which H_2 is produced from conventional sources such as natural gas and coal, or from alternative feedstocks such as glycerol, ethanol and methanol. The main catalytic reactions involved (i.e. steam reforming and WGS) are thermodynamically limited and therefore the in situ removal of CO_2 by a selective solid adsorbent lifts the equilibrium limitations and maximises the hydrogen productivity. Sorption-assistance can be applied either in the reforming/gasification unit or in the water gas shift stage, although thermodynamic studies indicate the convenience of enhancing the latter.

Sorption-enhancement is also regarded as an attractive pre-combustion CO_2 capture technology. Therefore, extensive research has focused on finding adequate CO_2 solid adsorbents that operate under the relevant operating condition of these applications. Layered double hydroxides, also known as hydrotalcites, are one of the most promising groups of adsorbents for the enhancement of the water gas shift reaction, showing high selectivity towards CO_2 at temperatures between 473 and 723 K. In addition, they are sulphur tolerant and their activity is favoured by the presence of water. Compared to other solid adsorbents, LDHs show faster kinetics and the energy needed in their regeneration is considerably lower. Despite all these positive characteristics, LDHs show relatively low adsorption capacities and their multicycle stability needs to be improved before they are widely used in sorption-enhanced H_2 production and in other CCS processes.

Among the different efforts to enhance the performance of LDHs, emphasis has been given to the improvement of the adsorption capacity (e.g. framework substitution and alkali promotion) and only few studies have tackled the development of more stable adsorbents. A very novel strategy to increase the intrinsic capacity of hydrotalcites is the use of high surface area materials as support. It is expected that the resulting hybrids will exhibit better stability, although this effect has been seldom explored. This thesis focuses on the development of LDHs supported on carbon structures and on the assessment of their performance as CO₂ adsorbents. The aim of the present study is to obtain stable materials with an adequate capacity per mass of total adsorbent. Pure and alkali promoted adsorbents were tested. For some relevant samples, the adsorption thermodynamics and kinetics were studied to assess their suitability for sorption-enhanced hydrogen production processes.

References

1. Yang, R. T. (1997). *Gas separation by adsorption processes* (Vol. 1). London, UK: Imperial College Press.
2. Ponec, V., Knor, Z., & Cerny, S. (1974). *Adsorption on solids*. Prague, Czech Republic: London Butterworths.
3. Ruthven, D. M. (1984). *Principles of adsorption and adsorption processes*. NY, USA: Wiley.
4. Suzuki, M. (1990). *Adsorption engineering*. Tokyo, Japan: Kodansha.
5. Ruthven, D. M., Farooq, S., & Knaebel, K. S. (1994). *Pressure swing adsorption*. NY, USA: VCH Publishers.
6. Do, D. D. (1998). *Adsorption analysis: Equilibria and Kinetics*. London, UK: Imperial College Press.
7. Rouquerol, F., Rouquerol, J., & Sing, K. (1999). *Adsorption by powders & porous solids*. London, UK: Academic Press.
8. Keller, J. U., & Staudt, R. (2005). *Gas adsorption equilibria: Experimental methods and adsorption isotherms*. Boston, USA: Springer.
9. Smith, J. M., Van Ness, H. C., & Abbott, M. M. (2001). *Introduction to chemical engineering thermodynamics*. London, UK: McGraw-Hill.
10. Sircar, S., Mohr, R., Ristic, C., & Rao, M. B. (1999). Isothermic heat of adsorption: Theory and experiment. *The Journal of Physical Chemistry B*, 103(31), 6539–6546.
11. Attard, G., & Barnes, C. (2009). *Surfaces* (Vol. 59). NY, USA: Oxford University Press.
12. Koumpouras, G. (2007). Mathematical modelling of a low temperature hydrogen production process with in situ CO₂ capture. Ph.D. thesis, Imperial College London, London, UK.
13. Vannice, M. A. (2005). *Kinetics of catalytic reactions*. PA, USA: Springer.
14. Huang, T.-C., & Cho, L.-T. (1989). Relationships between constants of the Freundlich equation and temperature for gaseous adsorption. *Chemical Engineering Communications*, 75(1), 181–194.
15. Halsey, G., & Taylor, H. S. (1947). The adsorption of hydrogen on tungsten powders. *The Journal of Chemical Physics*, 15(9), 624–630.
16. Belmabkhout, Y., Frère, M., & Weireld, G. D. (2004). High-pressure adsorption measurements. A comparative study of the volumetric and gravimetric methods. *Measurement Science & Technology*, 15(5), 848.
17. Capezzuoli, F. (2006). Carbon dioxide adsorption on porous materials and its catalytic hydrogenation in supercritical phase. Ph.D. thesis, Imperial College London, London, UK.

18. Hutson, N. D., & Attwood, B. C. (2008). High temperature adsorption of CO₂ on various hydrotalcite-like compounds. *Adsorption*, 14(6), 781–789.
19. Du, H., Ebner, A. D., & Ritter, J. A. (2010). Temperature dependence of the nonequilibrium kinetic model that describes the adsorption and desorption behavior of CO₂ in K-promoted HTlc. *Industrial and Engineering Chemistry Research*, 49(7), 3328–3336.
20. Choi, S., Drese, J. H., & Jones, C. W. (2009). Adsorbent materials for carbon dioxide capture from large anthropogenic point sources. *ChemSusChem*, 2(9), 796–854.
21. Wood, G. O. (2002). Quantification and application of skew of breakthrough curves for gases and vapors eluting from activated carbon beds. *Carbon*, 40(11), 1883–1890.
22. Soares, J., Casarin, G., José, H., Moreira, R. P. M., & Rodrigues, A. (2005). Experimental and theoretical analysis for the CO₂ adsorption on hydrotalcite. *Adsorption*, 11(1), 237–241.
23. Lee, K. B., Verdooren, A., Caram, H. S., & Sircar, S. (2007). Chemisorption of carbon dioxide on potassium-carbonate-promoted hydrotalcite. *Journal of Colloid and Interface Science*, 308(1), 30–39.
24. Kolade, M. A. (2008). Adsorptive reactor technology for VOC abatement. PhD thesis, Imperial College London, London, UK.
25. Halmann, M. M., & Steinberg, M. (1999). *Greenhouse gas carbon dioxide mitigation: Science and technology*. Boca Raton, FL: Lewis Publishers.
26. Yong, Z., Mata, V., & Rodrigues, A. R. E. (2002). Adsorption of carbon dioxide at high temperature—a review. *Separation and Purification Technology*, 26(2–3), 195–205.
27. Siriwardane, R. V., Shen, M.-S., Fisher, E. P., & Losch, J. (2005). Adsorption of CO₂ on zeolites at moderate temperatures. *Energy & Fuels*, 19(3), 1153–1159.
28. Xiao, P., Zhang, J., Webley, P., Li, G., Singh, R., & Todd, R. (2008). Capture of CO₂ from flue gas streams with zeolite 13X by vacuum-pressure swing adsorption. *Adsorption*, 14(4–5), 575–582.
29. Chen, C., Park, D.-W., & Ahn, W.-S. (2014). CO₂ capture using zeolite 13X prepared from bentonite. *Applied Surface Science*, 292, 63–67.
30. Guo, B., Chang, L., & Xie, K. (2006). Adsorption of carbon dioxide on activated carbon. *Journal of Natural Gas Chemistry*, 15(3), 223–229.
31. Drage, T. C., Blackman, J. M., Pevida, C., & Snape, C. E. (2009). Evaluation of activated carbon adsorbents for CO₂ capture in gasification. *Energy & Fuels*, 23(5), 2790–2796.
32. Yin, G., Liu, Z., Liu, Q., & Wu, W. (2013). The role of different properties of activated carbon in CO₂ adsorption. *Chemical Engineering Journal*, 230, 133–140.
33. Watabe, T., Nishizaka, Y., Kazama, S., & Yogo, K. (2013). Development of amine-modified solid sorbents for postcombustion CO₂ capture. *Energy Procedia*, 37, 199–204.
34. Dutcher, B., Fan, M., Cui, S., Shen, X.-D., Kong, Y., Russell, A. G., et al. (2013). Characterization and stability of a new, high-capacity amine-functionalized CO₂ sorbent. *International Journal of Greenhouse Gas Control*, 18, 51–56.
35. Le, Y., Guo, D., Cheng, B., & Yu, J. (2013). Amine-functionalized monodispersed porous silica microspheres with enhanced CO₂ adsorption performance and good cyclic stability. *Journal of Colloid and Interface Science*, 408, 173–180.
36. Yazaydin, A. Ö., Benin, A. I., Faheem, S. A., Jakubczak, P., Low, J. J., Willis, R. R., & Snurr, R. Q. (2009). Enhanced CO₂ adsorption in metal-organic frameworks via occupation of open-metal sites by coordinated water molecules. *Chemistry of Materials*, 21(8), 1425–1430.
37. Li, J.-R., Ma, Y., McCarthy, M. C., Sculley, J., Yu, J., Jeong, H.-K., et al. (2011). Carbon dioxide capture-related gas adsorption and separation in metal-organic frameworks. *Coordination Chemistry Reviews*, 255(15–16), 1791–1823.
38. Ye, S., Jiang, X., Ruan, L.-W., Liu, B., Wang, Y.-M., Zhu, J.-F., & Qiu, L.-G. (2013). Post-combustion CO₂ capture with the HKUST-1 and MIL-101(Cr) metal-organic frameworks: Adsorption, separation and regeneration investigations. *Microporous and Mesoporous Materials*, 179, 191–197.

39. Yong, Z., Mata, V., & Rodrigues, A. (2001). Adsorption of carbon dioxide on chemically modified high surface area carbon-based adsorbents at high temperature. *Adsorption*, 7(1), 41–50.
40. Xiao, P., Wilson, S., Xiao, G., Singh, R., & Webley, P. (2009). Novel adsorption processes for carbon dioxide capture within a IGCC process. *Energy Procedia*, 1(1), 631–638.
41. Lee, S. C., Chae, H. J., Lee, S. J., Choi, B. Y., Yi, C. K., Lee, J. B., et al. (2008). Development of regenerable MgO-based sorbent promoted with K_2CO_3 for CO_2 capture at low temperatures. *Environmental Science and Technology*, 42(8), 2736–2741.
42. Bhagiyalakshmi, M., Lee, J. Y., & Jang, H. T. (2010). Synthesis of mesoporous magnesium oxide: Its application to CO_2 chemisorption. *International Journal of Greenhouse Gas Control*, 4(1), 51–56.
43. Lee, K. B., Beaver, M. G., Caram, H. S., & Sircar, S. (2007). Chemisorption of carbon dioxide on sodium oxide promoted alumina. *AIChE Journal*, 53(11), 2824–2831.
44. Beaver, M., & Sircar, S. (2010). Adsorption technology for direct recovery of compressed, pure CO_2 from a flue gas without pre-compression or pre-drying. *Adsorption*, 16(3), 103–111.
45. Ding, Y., & Alpay, E. (2000). Equilibria and kinetics of CO_2 adsorption on hydrotalcite adsorbent. *Chemical Engineering Science*, 55(17), 3461–3474.
46. Yong, Z., & Rodrigues, A. R. E. (2002). Hydrotalcite-like compounds as adsorbents for carbon dioxide. *Energy Conversion and Management*, 43(14), 1865–1876.
47. Xiong, R., Ida, J., & Lin, Y. S. (2003). Kinetics of carbon dioxide sorption on potassium-doped lithium zirconate. *Chemical Engineering Science*, 58(19), 4377–4385.
48. Ochoa-Fernandez, E., Ronning, M., Yu, X., Grande, T., & Chen, D. (2007). Compositional effects of nanocrystalline lithium zirconate on its CO_2 capture properties. *Industrial and Engineering Chemistry Research*, 47(2), 434–442.
49. Iwan, A., Stephenson, H., Ketchie, W. C., & Lapkin, A. A. (2009). High temperature sequestration of CO_2 using lithium zirconates. *Chemical Engineering Journal*, 146(2), 249–258.
50. Solieman, A. A. A., Dijkstra, J. W., Haije, W. G., Cobden, P. D., & van den Brink, R. W. (2009). Calcium oxide for CO_2 capture: Operational window and efficiency penalty in sorption-enhanced steam methane reforming. *International Journal of Greenhouse Gas Control*, 3(4), 393–400.
51. Dou, B., Song, Y., Liu, Y., & Feng, C. (2010). High temperature CO_2 capture using calcium oxide sorbent in a fixed-bed reactor. *Journal of Hazardous Materials*, 183(1–3), 759–765.
52. Dean, C. C., Blamey, J., Florin, N. H., Al-Jeboori, M. J., & Fennell, P. S. (2011). The calcium looping cycle for CO_2 capture from power generation, cement manufacture and hydrogen production. *Chemical Engineering Research and Design*, 89(6), 836–855.
53. Hufton, J. R., Mayorga, S., & Sircar, S. (1999). Sorption-enhanced reaction process for hydrogen production. *AIChE Journal*, 45(2), 248–256.
54. Ding, Y., & Alpay, E. (2000). Adsorption-enhanced steam–methane reforming. *Chemical Engineering Science*, 55(18), 3929–3940.
55. van Selow, E. R., Cobden, P. D., Verbraeken, P. A., Hufton, J. R., & van den Brink, R. W. (2009). Carbon capture by sorption-enhanced water–gas shift reaction process using hydrotalcite-based material. *Industrial and Engineering Chemistry Research*, 48(9), 4184–4193.
56. Jang, H. M., Lee, K. B., Caram, H. S., & Sircar, S. (2012). High-purity hydrogen production through sorption enhanced water gas shift reaction using K_2CO_3 -promoted hydrotalcite. *Chemical Engineering Science*, 73, 431–438.
57. Cavani, F., Trifirò, F., & Vaccari, A. (1991). Hydrotalcite-type anionic clays: Preparation, properties and applications. *Catalysis Today*, 11(2), 173–301.
58. Rousselot, I., Taviot-Guého, C., Leroux, F., Léone, P., Palvadeau, P., & Besse, J.-P. (2002). Insights on the structural chemistry of hydrocalumite and hydrotalcite-like materials: Investigation of the series $Ca_2M^{3+}(OH)_6Cl \cdot 2H_2O$ (M^{3+} : Al^{3+} , Ga^{3+} , Fe^{3+} , and Sc^{3+}) by X-ray powder diffraction. *Journal of Solid State Chemistry*, 167(1), 137–144.

59. He, J., Wei, M., Li, B., Kang, Y., Evans, D. G., & Duan, X. (2006). *Layered double hydroxides* (Vol. 119). Heidelberg, Germany: Springer.
60. Othman, M. R., Helwani, Z., & Fernando, W. J. N. (2009). Synthetic hydrotalcites from different routes and their application as catalysts and gas adsorbents: A review. *Applied Organometallic Chemistry*, 23(9), 335–346.
61. León, M., Díaz, E., Bennici, S., Vega, A., Ordóñez, S., & Auroux, A. (2010). Adsorption of CO₂ on hydrotalcite-derived mixed oxides: Sorption mechanisms and consequences for adsorption irreversibility. *Industrial and Engineering Chemistry Research*, 49(8), 3663–3671.
62. Gao, Y., Zhang, Z., Wu, J., Yi, X., Zheng, A., Umar, A., et al. (2013). Comprehensive investigation of CO₂ adsorption on Mg-Al-CO₃ LDH-derived mixed metal oxides. *Journal of Materials Chemistry A*, 1(41), 12782–12790.
63. Debecker, D. P., Gaigneaux, E. M., & Busca, G. (2009). Exploring, tuning, and exploiting the basicity of hydrotalcites for applications in heterogeneous catalysis. *Chemistry—A European Journal*, 15(16), 3920–3935.
64. Ebner, A. D., Reynolds, S. P., & Ritter, J. A. (2006). Understanding the adsorption and desorption behavior of CO₂ on a K-promoted hydrotalcite-like compound (HTlc) through nonequilibrium dynamic isotherms. *Industrial and Engineering Chemistry Research*, 45(18), 6387–6392.
65. Ram Reddy, M. K., Xu, Z. P., Lu, G. Q., & Diniz da Costa, J. C. (2006). Layered double hydroxides for CO₂ capture: Structure evolution and regeneration. *Industrial & Engineering Chemistry Research*, 45(22), 7504–7509.
66. Wang, X. P., Yu, J. J., Cheng, J., Hao, Z. P., & Xu, Z. P. (2007). High-temperature adsorption of carbon dioxide on mixed oxides derived from hydrotalcite-like compounds. *Environmental Science and Technology*, 42(2), 614–618.
67. Hutson, N. D., Speakman, S. A., & Payzant, E. A. (2004). Structural effects on the high temperature adsorption of CO₂ on a synthetic hydrotalcite. *Chemistry of Materials*, 16(21), 4135–4143.
68. Turco, M., Bagnasco, G., Costantino, U., Marmottini, F., Montanari, T., Ramis, G., & Busca, G. (2004). Production of hydrogen from oxidative steam reforming of methanol: I. Preparation and characterization of Cu/ZnO/Al₂O₃ catalysts from a hydrotalcite-like LDH precursor. *Journal of Catalysis*, 228(1), 43–55.
69. Pérez-Ramírez, J., Abelló, S., & van der Pers, N. M. (2007). Memory effect of activated Mg–Al hydrotalcite: In Situ XRD studies during decomposition and gas-phase reconstruction. *Chemistry—A European Journal*, 13(3), 870–878.
70. Di Cosimo, J. I., Díez, V. K., & Apesteguía, C. R. (1996). Base catalysis for the synthesis of α , β -unsaturated ketones from the vapor-phase aldol condensation of acetone. *Applied Catalysis, A: General*, 137(1), 149–166.
71. Tichit, D., & Coq, B. (2003). Catalysis by hydrotalcites and related materials. *CATTECH*, 7(6), 206–217.
72. Climent, M. J., Corma, A., Iborra, S., Epping, K., & Velt, A. (2004). Increasing the basicity and catalytic activity of hydrotalcites by different synthesis procedures. *Journal of Catalysis*, 225(2), 316–326.
73. Abelló, S., Medina, F., Tichit, D., Pérez-Ramírez, J., Groen, J. C., Sueiras, J. E., et al. (2005). Aldol condensations over reconstructed Mg–Al hydrotalcites: Structure-activity relationships related to the rehydration method. *Chemistry—A European Journal*, 11(2), 728–739.
74. Hibino, T., Yamashita, Y., Kosuge, K., & Tsunashima, A. (1995). Decarbonation behavior of Mg–Al–CO₃ hydrotalcite-like compounds during heat treatment. *Clays and Clay Minerals*, 43(4), 427–432.
75. Yong, Z., Mata, V., & Rodrigues, A. E. (2000). Adsorption of carbon dioxide onto hydrotalcite-like compounds (HTlcs) at high temperatures. *Industrial and Engineering Chemistry Research*, 40(1), 204–209.

76. Yang, W., Kim, Y., Liu, P. K. T., Sahimi, M., & Tsotsis, T. T. (2002). A study by in situ techniques of the thermal evolution of the structure of a Mg–Al–CO₃ layered double hydroxide. *Chemical Engineering Science*, 57(15), 2945–2953.
77. Auroux, A., & Gervasini, A. (1990). Microcalorimetric study of the acidity and basicity of metal oxide surfaces. *The Journal of Physical Chemistry*, 94(16), 6371–6379.
78. Philipp, R., & Fujimoto, K. (1992). FTIR spectroscopic study of carbon dioxide adsorption/desorption on magnesia/calcium oxide catalysts. *The Journal of Physical Chemistry*, 96(22), 9035–9038.
79. Di Cosimo, J. I., Díez, V. K., Xu, M., Iglesia, E., & Apesteguía, C. R. (1998). Structure and surface and catalytic properties of Mg–Al basic oxides. *Journal of Catalysis*, 178(2), 499–510.
80. Meis, N. N. A. H., Bitter, J. H., & de Jong, K. P. (2009). Support and size effects of activated hydrotalcites for precombustion CO₂ capture. *Industrial and Engineering Chemistry Research*, 49(3), 1229–1235.
81. Tsuji, M., Mao, G., Yoshida, T., & Tamaura, Y. (1993). Hydrotalcites with an extended Al³⁺-substitution: Synthesis, simultaneous TG-DTA-MS study, and their CO₂ adsorption behaviors. *Journal of Materials Research*, 8(05), 1137–1142.
82. White, M., Iretski, A., Weigel, S., Chiang, R., & Brozozowski, J. (2006). *Adsorbents, methods of preparation, and methods of use thereof*. Google Patents.
83. Yavuz, C. T., Shinall, B. D., Iretskii, A. V., White, M. G., Golden, T., Atilhan, M., et al. (2009). Markedly improved CO₂ capture efficiency and stability of gallium substituted hydrotalcites at elevated temperatures. *Chemistry of Materials*, 21(15), 3473–3475.
84. Wang, Q., Tay, H. H., Ng, D. J. W., Chen, L., Liu, Y., Chang, J., et al. (2010). The effect of trivalent cations on the performance of Mg–M–CO₃ layered double hydroxides for high-temperature CO₂ capture. *ChemSusChem*, 3(8), 965–973.
85. Reijers, H. T. J., Valster-Schiermeier, S. E. A., Cobden, P. D., & van den Brink, R. W. (2005). Hydrotalcite as CO₂ sorbent for sorption-enhanced steam reforming of methane. *Industrial and Engineering Chemistry Research*, 45(8), 2522–2530.
86. Yang, J.-I., & Kim, J.-N. (2006). Hydrotalcites for adsorption of CO₂ at high temperature. *Korean Journal of Chemical Engineering*, 23(1), 77–80.
87. Abelló, S., Medina, F., Tichit, D., Pérez-Ramírez, J., Rodríguez, X., Sueiras, J. E., et al. (2005). Study of alkaline-doping agents on the performance of reconstructed Mg–Al hydrotalcites in aldol condensations. *Applied Catalysis, A: General*, 281(1–2), 191–198.
88. Meis, N. N. A. H., Bitter, J. H., & de Jong, K. P. (2010). On the influence and role of alkali metals on supported and unsupported activated hydrotalcites for CO₂ sorption. *Industrial and Engineering Chemistry Research*, 49(17), 8086–8093.
89. Ebner, A. D., Reynolds, S. P., & Ritter, J. A. (2007). Nonequilibrium kinetic model that describes the reversible adsorption and desorption behavior of CO₂ in a K-promoted hydrotalcite-like compound. *Industrial and Engineering Chemistry Research*, 46(6), 1737–1744.
90. Oliveira, E. L. G., Grande, C. A., & Rodrigues, A. E. (2008). CO₂ sorption on hydrotalcite and alkali-modified (K and Cs) hydrotalcites at high temperatures. *Separation and Purification Technology*, 62(1), 137–147.
91. Walspurger, S., Boels, L., Cobden, P. D., Elzinga, G. D., Haije, W. G., & van den Brink, R. W. (2008). The crucial role of the K⁺–aluminium oxide interaction in K⁺-promoted alumina- and hydrotalcite-based materials for CO₂ sorption at high temperatures. *ChemSusChem*, 1(7), 643–650.
92. Wu, Y. J., Li, P., Yu, J. G., Cunha, A. F., & Rodrigues, A. E. (2013). K-Promoted hydrotalcites for CO₂ capture in sorption enhanced reactions. *Chemical Engineering and Technology*, 36(4), 567–574.
93. Ding, Y., & Alpay, E. (2001). High temperature recovery of CO₂ from flue gases using hydrotalcite adsorbent. *Process Safety and Environmental Protection*, 79(1), 45–51.

94. Ram Reddy, M. K., Xu, Z. P., & Diniz da Costa, J. C. (2008). Influence of water on high-temperature CO₂ capture using layered double hydroxide derivatives. *Industrial & Engineering Chemistry Research*, 47(8), 2630–2635.
95. van Dijk, H. A. J., Walspurger, S., Cobden, P. D., van den Brink, R. W., & de Vos, F. G. (2011). Testing of hydrotalcite-based sorbents for CO₂ and H₂S capture for use in sorption enhanced water gas shift. *International Journal of Greenhouse Gas Control*, 5(3), 505–511.
96. Othman, M. R., Rasid, N. M., & Fernando, W. J. N. (2006). Mg–Al hydrotalcite coating on zeolites for improved carbon dioxide adsorption. *Chemical Engineering Science*, 61(5), 1555–1560.
97. Aschenbrenner, O., McGuire, P., Alsamaq, S., Wang, J., Supasitmongkol, S., Al-Duri, B., et al. (2011). Adsorption of carbon dioxide on hydrotalcite-like compounds of different compositions. *Chemical Engineering Research and Design*, 89(9), 1711–1721.
98. Tessonnier, J. P. (2009). Carbon materials in heterogeneous catalysis. In Planck, F.-M. (Ed.), *Lecture series: Modern methods in heterogeneous catalysis*.
99. Chinthaginjala, J. K., Seshan, K., & Lefferts, L. (2007). Preparation and application of carbon-nanofiber based microstructured materials as catalyst supports. *Industrial and Engineering Chemistry Research*, 46(12), 3968–3978.
100. Wong, H. S. P., & Akinwande, D. (2011). *Carbon nanotube and graphene device physics*. NY, USA: Cambridge University Press.
101. Rakov, E. G. (2006). *Nanotubes and nanofibers*. FL, USA: Taylor and Francis Group.
102. Machado, B. F., & Serp, P. (2012). Graphene-based materials for catalysis. *Catalysis Science & Technology*, 2(1), 54–75.
103. Lerf, A., He, H., Forster, M., & Klinowski, J. (1998). Structure of graphite oxide revisited. *The Journal of Physical Chemistry B*, 102(23), 4477–4482.
104. Olah, G. A., Goeppert, A., & Prakash, G. K. S. (2006). *Beyond oil and gas: The methanol economy*. Weinheim, Germany: Wiley-VCH.
105. Baade, W. F., Parekh, U. N., & Raman, V. S. (2001). *Hydrogen* (Vol. 13, pp. 759–808). Kirk-Othmer Encyclopedia (online).
106. Rostrup-Nielsen, J. R. (2008). Steam reforming. In *Handbook of heterogeneous catalysis*. Weinheim: Wiley-VCH Verlag GmbH & Co. KGaA.
107. Harrison, D. P. (2008). Sorption-enhanced hydrogen production: A review. *Industrial and Engineering Chemistry Research*, 47(17), 6486–6501.
108. Nielsen, P. E. H., Hansen, J. B., & Schiødt, N. C. (2009). Process for the preparation of a hydrogen-rich stream. US 7,527,781 B2.
109. Choi, Y., & Stenger, H. (2002). Kinetics of methanol decomposition and water gas shift reaction on a commercial Cu-ZnO/Al₂O₃ catalyst. *Fuel Chemistry Division Preprints*, 47, 723–724.
110. Carvill, B. T., Hufton, J. R., Anand, M., & Sircar, S. (1996). Sorption-enhanced reaction process. *AIChE Journal*, 42(10), 2765–2772.
111. Reijers, H. T. J., Boon, J., Elzinga, G. D., Cobden, P. D., Haije, W. G., & Brink, R. W. V. D. (2009). Modeling study of the sorption-enhanced reaction process for CO₂ capture. II. Application to steam-methane reforming. *Industrial & Engineering Chemistry Research*, 48(15), 6975–6982.
112. Broda, M., Manovic, V., Imtiaz, Q., Kierzkowska, A. M., Anthony, E. J., & Müller, C. R. (2013). High-purity hydrogen via the sorption-enhanced steam methane reforming reaction over a synthetic CaO-based sorbent and a Ni catalyst. *Environmental Science and Technology*, 47(11), 6007–6014.
113. Ochoa-Fernandez, E., Haugen, G., Zhao, T., Ronning, M., Aartun, I., Borresen, B., et al. (2007). Process design simulation of H₂ production by sorption enhanced steam methane reforming: evaluation of potential CO₂ acceptors. *Green Chemistry*, 9(6), 654–662.
114. van Selow, E. R., Cobden, P. D., van den Brink, R. W., Hufton, J. R., & Wright, A. (2009). Performance of sorption-enhanced water-gas shift as a pre-combustion CO₂ capture technology. *Energy Procedia*, 1(1), 689–696.

115. Stevens, R. W., Jr., Shamsi, A., Carpenter, S., & Siriwardane, R. (2010). Sorption-enhanced water gas shift reaction by sodium-promoted calcium oxides. *Fuel*, 89(6), 1280–1286.
116. Liu, Y., Li, Z., Xu, L., & Cai, N. (2012). Effect of sorbent type on the sorption enhanced water gas shift process in a fluidized bed reactor. *Industrial and Engineering Chemistry Research*, 51(37), 11989–11997.
117. Florin, N. H., & Harris, A. T. (2008). Enhanced hydrogen production from biomass with in situ carbon dioxide capture using calcium oxide sorbents. *Chemical Engineering Science*, 63(2), 287–316.
118. Pimenidou, P., Rickett, G., Dupont, V., & Twigg, M. V. (2010). High purity H₂ by sorption-enhanced chemical looping reforming of waste cooking oil in a packed bed reactor. *Bioresource technology*, 101(23), 9279–9286.
119. Chen, H., Zhang, T., Dou, B., Dupont, V., Williams, P., Ghadiri, M., & Ding, Y. (2009). Thermodynamic analyses of adsorption-enhanced steam reforming of glycerol for hydrogen production. *International Journal of Hydrogen Energy*, 34(17), 7208–7222.
120. Dou, B., Rickett, G. L., Dupont, V., Williams, P. T., Chen, H., Ding, Y., & Ghadiri, M. (2010). Steam reforming of crude glycerol with in situ CO₂ sorption. *Bioresource technology*, 101(7), 2436–2442.
121. Comas, J., Laborde, M., & Amadeo, N. (2004). Thermodynamic analysis of hydrogen production from ethanol using CaO as a CO₂ sorbent. *Journal of Power Sources*, 138(1–2), 61–67.
122. He, L., Berntsen, H., & Chen, D. (2009). Approaching sustainable H₂ production: Sorption enhanced steam reforming of ethanol. *The Journal of Physical Chemistry A*, 114(11), 3834–3844.
123. Li, M. (2009). Thermodynamic analysis of adsorption enhanced reforming of ethanol. *International Journal of Hydrogen Energy*, 34(23), 9362–9372.
124. Cobden, P. D., van Beurden, P., Reijers, H. T. J., Elzinga, G. D., Kluiters, S. C. A., Dijkstra, J. W., et al. (2007). Sorption-enhanced hydrogen production for pre-combustion CO₂ capture: Thermodynamic analysis and experimental results. *International Journal of Greenhouse Gas Control*, 1(2), 170–179.

Supported Layered Double Hydroxides as CO₂
Adsorbents for Sorption-enhanced H₂ Production

Iruretagoyena Ferrer, D.

2016, XXXVII, 209 p. 96 illus., 94 illus. in color.,

Hardcover

ISBN: 978-3-319-41275-7